Characterization of graphene-rubber nanocomposites: a review

Sayfo P., Pirityi D. Z., Pölöskei K.

Accepted for publication in MATERIALS TODAY CHEMISTRY
Published in 2023
DOI: 10.1016/j.mtchem.2023.101397

Materials Today Chemistry 29 (2023) 101397

Contents lists available at ScienceDirect

Materials Today Chemistry

journal homepage: www.journals.elsevier.com/materials-today-chemistry/

Characterization of graphene-rubber nanocomposites: a review

P. Sayfo, D.Z. Pirityi, K. Pölöskei*

Department of Polymer Engineering, Faculty of Mechanical Engineering, Budapest University of Technology and Economics, Műegyetem Rkp. 3., Budapest H-1111, Hungary

ARTICLE INFO

Article history:
Received 25 October 2022
Received in revised form
27 December 2022
Accepted 12 January 2023
Available online xxx

Keywords:
Graphene
Graphene oxide
Nanoparticle
Nanocomposite
Elastomer
Rubber

ABSTRACT

Since its discovery in 2004, graphene has gained significant attention from both industry and academia. Its unique properties enable us to produce novel, enhanced polymer composites contributing to environmental and economic benefits. Graphene can improve the abrasion resistance of materials; thus, it can increase the service life of rubber tires. This present review discusses the testing of key properties of graphene and its elastomeric nanocomposites from a practical point of view. Graphene's layer thickness and its oxygen content are two key factors determining nano reinforcement's success. It is vital to monitor these properties both before and after mixing graphene with rubber to guarantee the high quality of the resulting nanocomposites. Ultimately, the distribution of nanoparticles within the matrix also plays a vital role in assuring strong reinforcement. Overall, we found that X-ray diffraction (XRD) spectroscopy can detect variation in all three aspects. Furthermore, Raman spectroscopy, transmission electron microscopy (TEM), and energy dispersive spectroscopy (EDS) can be used complementarily to support XRD findings.

1. Introduction

Graphene is a single-layer allotrope of carbon, which has a hexagonal lattice structure consisting of carbon atoms with sp^2 hybridization. It is regarded as one of the most exciting material science discoveries of the 21st century yet. It has been steadily gaining popularity and importance over the past 10–15 years. It was first isolated by Andre Geim and Konstantin Novoselov in 2004. They separated graphite's layers using adhesive tapes [1], for which they were awarded the Nobel Prize in Physics in 2010. Since then, graphene has attracted the interest of several industries because of its unique technical properties. It can be the basis for many innovative solutions in electronics [2–7], healthcare [8–14], energetics [15–20], filtration technology [21–24], polymer science [25–29], and other fields.

Graphene (along with single-wall carbon nanotubes) has the highest Young's modulus of all known materials (around 1 TPa) [30], while its estimated specific surface area is 2630 m^2/g [31]. These properties ensure that graphene is an effective reinforcing material. Due to its molecular structure, it is compatible with non-polar organic polymers.

Since 2004, graphene production methods have been developed, and a wide range of options are now available, yet costs are still too high for their widespread industrial introduction. Graphene can be produced via micromechanical or ultrasonic exfoliation [32], chemical vapor deposition (CVD) [33], oxidation-reduction pathways via graphene oxide (GO) intermediate [34–37], the cathodic electrolysis of graphite [38,39], and the intercalation of organic solvents (i.e. tetrahydrofuran) between graphite layers and subsequent thermal exfoliation [40,41]. The quality of graphene depends on its production technology, which affects its price and field of application [33,42].

In scientific literature, the term 'graphene' is freely used, in many cases deviating from the original definition of a 'single atomic layer of graphite'. During the production of graphene, several other derivates are also produced, such as graphene oxide (GO), reduced graphene oxide (rGO), and few-layer graphene (FLG). In this paper, these terms are used according to Bianco et al.'s recommendations and the ISO/TS 80004-13:2017 standard [43,44]:

- Graphene is a single layer of carbon atoms arranged in a honeycomb structure. Though solid, it does not constitute a solid carbon material but is either suspended in a liquid or adhered to a foreign substrate;
- Graphene oxide (GO) is a chemically modified two-dimensional material prepared via the oxidation and subsequent exfoliation

* Corresponding author.
E-mail address: poloskei@pt.bme.hu (K. Pölöskei).

https://doi.org/10.1016/j.mtchem.2023.101397
2468-5194/

of graphite. It is often characterized by its carbon/oxygen atomic ratio (C/O ratio), which is approximately 2.0 depending on its preparation method;
- Reduced graphene oxide (rGO) is a two-dimensional material prepared via the reduction of GO, which would ideally yield graphene. However, the oxygen content cannot be eliminated, and the honeycomb structure may also get damaged. Reduction methods include chemical, thermal, microwave, photochemical, photo-thermal, and microbial technologies;
- Few-layer graphene (FLG) is a two-dimensional material with fewer than 10 well-defined graphene layers;
- Graphene nanoplatelets (GNP) are similar to FLG with thickness between 1 nm and 3 nm and lateral dimensions between 100 nm and 100 μm.

Even before the discovery of graphene, carbon derivates (i.e. carbon nanotubes, carbon fiber, or carbon black) were already widely used in the polymer industry. Among these, carbon black's importance stands out, especially in the rubber tire industry, with its annual consumption reaching 17 million tons by 2030 [45]. The high consumption of carbon black raises the question of whether there is an alternative reinforcing material that could replace it while maintaining or possibly improving the properties of rubber products. Nanoparticles, including graphene, and the nanocomposites produced from them offer such an opportunity. Their superior mechanical properties can be explained by their size effect. At the nano scale, materials often contain single crystals rather than bulk structures, hence voids, dislocations or microcracks are absent. Material properties are strongly dependent on characteristic particle size at the nanoscale. At increasing particle sizes these properties will tend to those of bulk materials [46]. Nanoparticles also have significantly higher surface to volume ratio than conventional macrostructures. Consequently, nanocomposites contain a higher amount of interfacial regions compared to conventional composites, leading to more efficient stress transfer between the phases [47,48]. This makes them more effective in improving mechanical properties at the same concentration in composites. However, nanoparticles' high tendency for aggregation makes them more difficult to disperse than regular fillers, especially at high concentrations [47,49].

The use of graphene and its derivatives as reinforcement in elastomers can significantly improve the abrasion resistance, modulus, and other mechanical properties of rubber products. Furthermore, even low concentrations of graphene can be enough to enhance these properties. While rubber tires contain up to 100 phr of carbon black, even 5 phr of graphene may be enough to achieve similar performance in ideal conditions. However, care must be taken to avoid the aggregation of nanoparticles to achieve optimal properties [50–56].

Extensive research has been conducted on how graphene-based nanoparticles affect various properties of rubbers. In general, graphene-based particles can change properties by several orders of magnitude even at concentrations below 1 phr. The percolation threshold of the nanocomposites is an important factor to consider. Once graphene forms a single interconnected secondary network in the composite, additional amounts no longer have such strong influence on material properties [57]. By introducing graphene into rubber, the polymer's intrinsic electric resistance can be canceled, thus it gives way for the production of dissipative or even conductive elastomers. The introduction of highly dispersed graphene can increase the electric conductivity of rubber by up to 10 orders of magnitude. It has been shown that aggregated graphene particles also have similar effects, but only at larger quantities, as their percolation threshold is considerably higher [58,59]. Analogously, graphene can increase the thermal conductivity of rubber by up to 50%. It has been shown that the presence of a π-conjugated structure is essential for this property, so graphene oxide is not suitable for this application. If the properties resulting from the addition of graphene are desirable except for thermal conductivity, foaming agents may also be applied to counteract its effects [60–62]. Graphene enhances the gas barrier properties of rubbers as well. It has been shown that oxygen permeability can be reduced by up to 80% at 5–10 phr of graphene content. This improvement can be attributed to a percolated, defect-free graphene structure that shuts off otherwise penetrable diffusion routes for gas molecules [63,64]. Electromagnetic shielding is also an important application of graphene nanoparticles. This property is heavily influenced by the dispersion and the concentration of the filler in the matrix. Up to 45 dB of shielding is attainable at 5–10 phr of graphene content and 2 mm sample thickness [62,65–67].

Graphene production is primarily evaluated based on particle thickness (i.e. number of layers). Also, in the case of the oxidation-reduction methods, graphene's oxygen content is an important characteristic. Consequently, these properties of graphene must be determined to ensure its successful application in elastomeric nanocomposites. At the moment, there is no standardized testing procedure available for these properties. Conclusions can be drawn only from the combination of several analytic tools. It is necessary to present their advantages, and disadvantages and how they can be applied to these specific needs. The vast majority of them are spectroscopic and microscopic techniques widely used in modern analytics.

2. Testing methods for nanoparticle size and thickness

Graphene consists of flat, sheet-like particles, having much larger extents in two dimensions than in the third one. Graphene's potential adhesion and reinforcing performance in polymer matrices heavily depend on its particle size distribution and specific surface area. Several techniques are overviewed in this chapter that can quantify the size and thickness of graphene particles.

2.1. Atomic force microscopy (AFM)

AFM can be used to scan the surface of a solid specimen. This method gives information about a small part of the top atomic layers of a sample. Consequently, many images must be taken for this technique to yield reliable, representative results. There are several AFM images of graphene samples in the scientific literature. Using this method, it is possible to determine the layer thickness of graphene particles.

There are two common strategies for the determination of particle thickness with AFM. The easiest way is to perform a surface analysis at the edge of an individual particle (Fig. 1b) [68]. Another possibility is to prepare a coating layer on the particles (i.e. by spin coating [69], electrophoretic deposition [59,60,70,71], or CVD [72]). This coating can be partially removed by laser [69], and the resulting cross-section can be examined (Fig. 1a). However, it should be noted that the removal of the coating may result in an increase in the coating thickness at the boundary of the part not removed. Therefore, a baseline at around 10 nm should be used to accurately determine graphene thickness [69].

The advantage of AFM is its small size and relatively low cost. The disadvantage is the long testing time, considering that multiple images are needed for each sample. Sample preparation requires special care because even the slightest contamination can undermine the measurement.

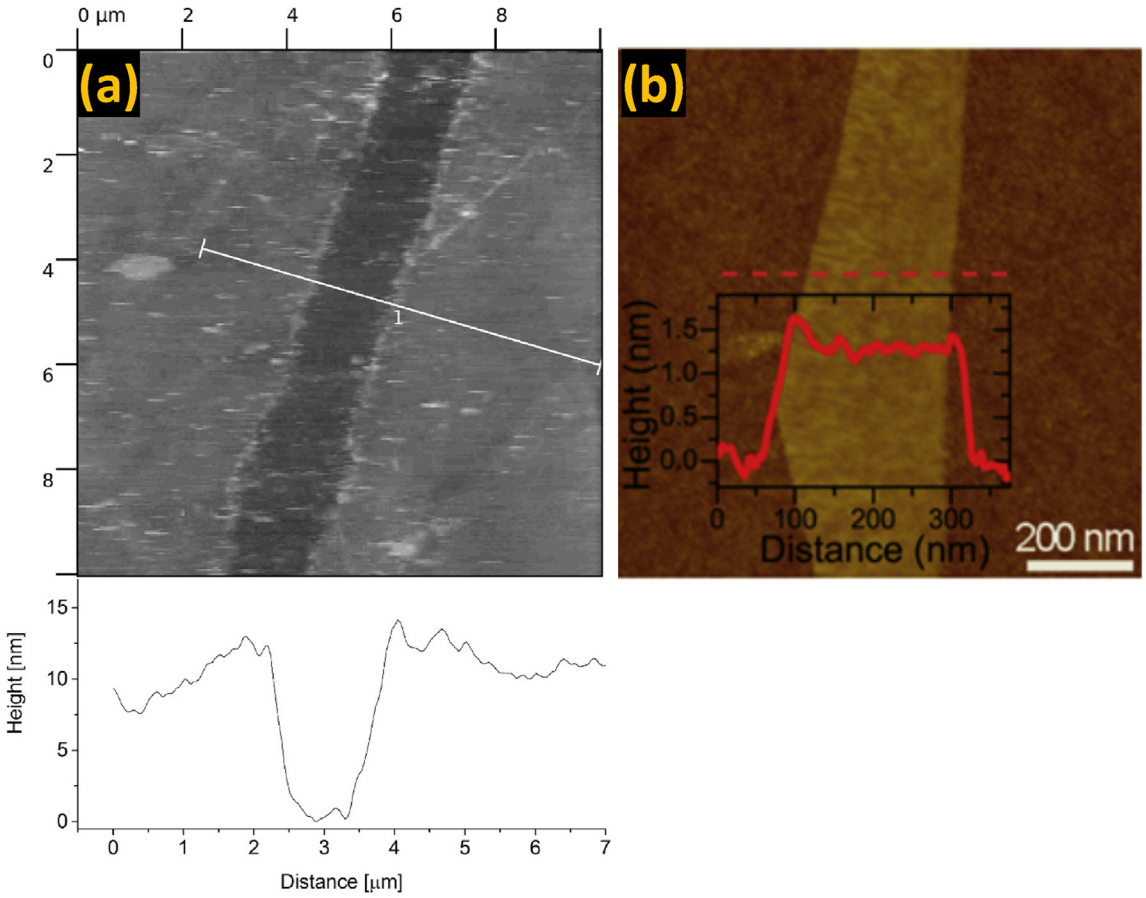

Fig. 1. AFM image, a) taken after GO coating and its laser removal to determine thickness. The white line shows the direction of the cross-section [69], b) the single layer graphene with (inset) cross section graph [68].

2.2. Raman spectroscopy

Raman spectroscopy is an analytical technique used to identify polarizable molecular bonds. The movements of delocalized π electrons in graphene are limited to the 2D graphene layer. In contrast, delocalized π electrons in graphite can move freely between different layers, allowing 3D movements. Increasing the number of layers in graphene from a single layer to multiple layers, the motion vector component, which is perpendicular to the graphene plane for delocalized electrons, is also increased. On the Raman spectra of single-layer or few-layer graphene, the characteristic peak around 2700 cm^{-1} corresponds to the motion of delocalized electrons perpendicular to the graphene plane (Fig. 2). This peak gets wider or broken into several smaller peaks as the number of graphene layers increases [73–85]. In the case of single-layer graphene the peak around 2700 cm^{-1} has a bandwidth of approximately 50.7 cm^{-1}, and the intensity ratio of the two peaks mentioned is about 1.11 [86]. Although this method is hardly applicable for identifying the exact number of layers in few-layer graphene samples, it is useful for proving whether the production of single-layer graphene was successful [86].

2.3. Scanning electron microscopy (SEM)

SEM is widely used in morphological studies. Since graphene and graphite are electrically conductive materials, there is no need to apply a conductive coating during sample preparation. The SEM images can visualize the shape of the particles and provide an approximation of their size distribution; it can also detect the degree of aggregation [74,77–97].

The SEM image of a typical graphene sample is shown in Fig. 3. To study the particle size distribution, numerous SEM images have to be taken, which can be a time-consuming task [75].

In addition, it must be taken into account that graphene particles are typically one to a few atoms thick. This thickness cannot be determined by SEM with the same accuracy as their lateral extent. An advantage of SEM is that it can be combined with energy dispersive spectroscopy (EDS) to obtain the C/O ratio.

2.4. Transmission electron microscopy (TEM)

The morphology of an ultrathin cross-section of any material can be analyzed by TEM. It is therefore ideal for determining the lateral extent of graphene particles [34,57,70,79,81–83, 87–94,98–104]. On the other hand, the thickness of graphene sheets is close to the resolution of TEM (0.1–0.2 nm), so its use for the determination of particle thickness is constrained.

Fig. 4 shows TEM images of GO (prepared via Hummer's method) and rGO (reduced with NaHS) particles. It can be seen that both samples have layered structures, but the reduction process has caused the layers to separate. The TEM images were used to support and confirm findings from other measurement methods (i.e. X-ray diffraction, Fourier transform infrared and UV-VIS-NIR spectroscopies) [37].

Lu et al. irradiated graphite by a high current pulsed electron beam to produce graphene [105]. With this method, the outer

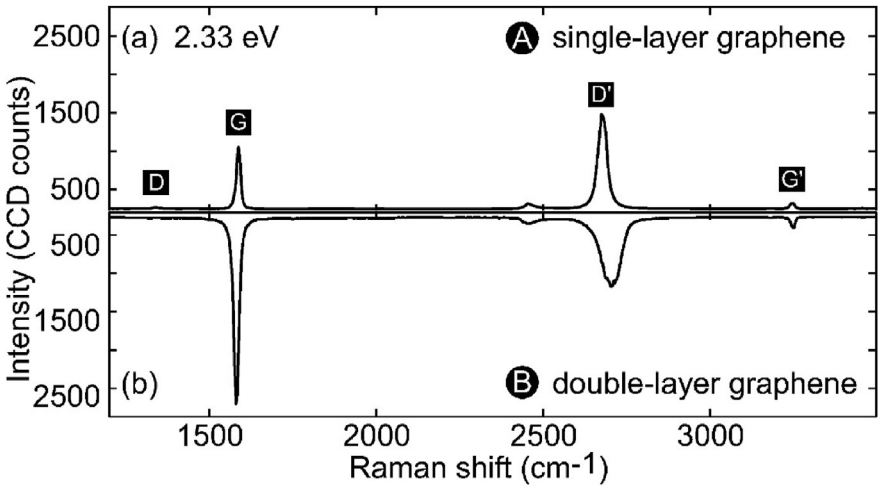

Fig. 2. Raman spectra of single layer and double layer graphene [73].

10 μm thick layer of the graphite particles exfoliated to FLG and/or graphene nanosheets. TEM images of the pristine graphite and the so produced graphene are shown in Fig. 5.

Since the preparation of pure graphene or GO samples for TEM can be complex, it is advisable to embed them in some matrix before the test.

2.5. X-ray diffraction (XRD)

XRD shows a clear difference between graphite, graphene, and GO samples. This analytical method provides information about crystallinity, i.e. periodic regularity in the sample. In the XRD spectrum of graphite, a single narrow peak at 26.4° is shown, corresponding to the spacing of the graphite crystal layers (Fig. 6a). In several cases, a second, smaller peak appears at around 54°, corresponding to double the distance between layers. Due to the incorporation of oxygen-containing functional groups during oxidation, the originally 0.335 nm layer spacing in graphite almost doubles in graphite oxide. However, oxygen-containing functional groups are formed randomly, so this increase does not appear uniformly everywhere. The layer spacing generally becomes 0.6–1 nm, resulting in a broadened peak on XRD spectra [35,96,106]. Furthermore, with increasing oxidation, the characteristic peak of graphite is shifted towards lower diffraction angles (Fig. 6b). After reduction, the layer spacing is no longer provided by the oxygen-containing functional groups, so graphene particles are allowed to arrange in a structure similar to graphite. The extent of this arrangement can be monitored by XRD [34,41,70,74,77,78,81,85–89,96–103,107–113]. With an increasing strain in the hexagonal structure of graphene, the peak can also slightly shift to lower diffraction angles. However, in this case, the difference is more likely to be found in the irregular shape of the peak, caused by the strain [114]. XRD can also be useful in cases when the goal is to produce FLG. In such cases, a graphite-like peak must be present in the XRD spectrum of the sample for the process to be successful.

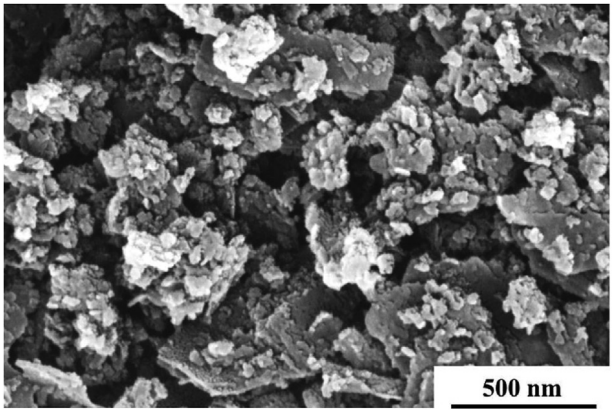

Fig. 3. SEM image of graphene powder synthesized by an ultrasonically assisted electrochemical exfoliation method [39].

3. Testing methods for oxygen content (in nano reinforcement or nanocomposite)

The simplest way to determine the oxidation degree of graphene is to evaluate the molar ratio of carbon and oxygen atoms (C/O) [115]. Its reciprocal (O/C) is also widely used in literature, but we chose to consistently use C/O in this review, according to the ISO/TS 80004-13:2017 standard [44]. In the present chapter, we discuss the most promising techniques used for this purpose.

3.1. Fourier-transform infrared spectroscopy (FTIR)

FTIR is a commonly used analytical technique to identify functional groups present in the analyte. With this method, information about the occurring functional groups in the sample can be gathered. Therefore, FTIR is frequently used for checking the success of preparing or reducing GO. Neither graphite nor pure graphene contains any oxygen, so their FTIR spectrum is almost flat; no characteristic peaks to oxygen-containing functional groups can be observed.

In GO, the following oxygen-containing functional groups occur: hydroxyl, carbonyl, carboxyl, and epoxy groups. Consequently, their corresponding characteristic peaks appear on the FTIR spectra of GO samples. The most relevant peaks are located at the wavenumbers specified in Table 1. The number of oxygen-containing functional groups is decreased during the reduction of GO to rGO. Thus, the respective peaks on the FTIR spectrum also become smaller or completely disappear (Fig. 7). Ideally, all oxygen-containing functional groups are reduced, and the product can be called graphene, but the restored aromatic structure must be proven with other analytic tools [52,78,79,88,89,97,106–109,116–119].

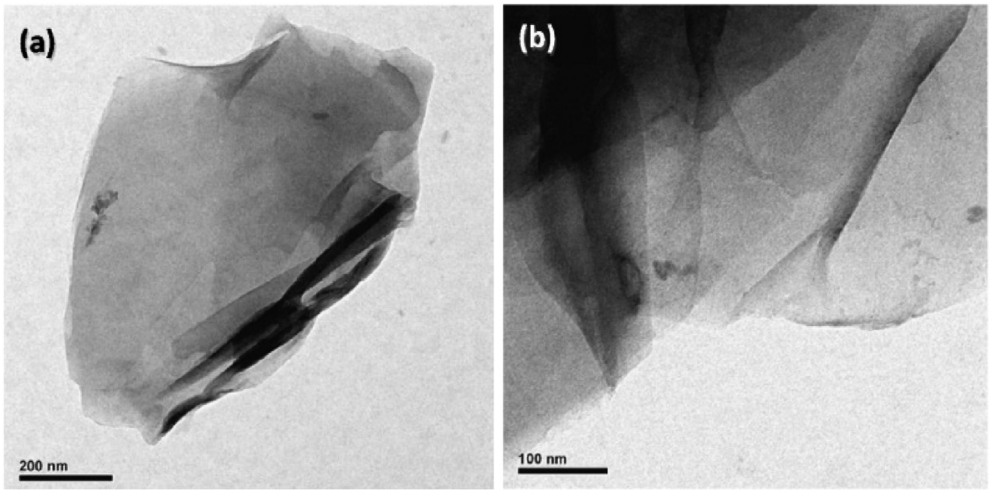

Fig. 4. TEM images of a) GO, b) rGO [37].

The use of FTIR for graphene quality control is not limited to cases when graphene is produced via traditional oxidation-reduction pathways. An example of this is shown in Fig. 8. Pingale et al. produced graphene via the electrolysis of graphite [39]. However, as shown in the FTIR spectrum, graphene was accidentally oxidized by the acidic environment. In such cases, the

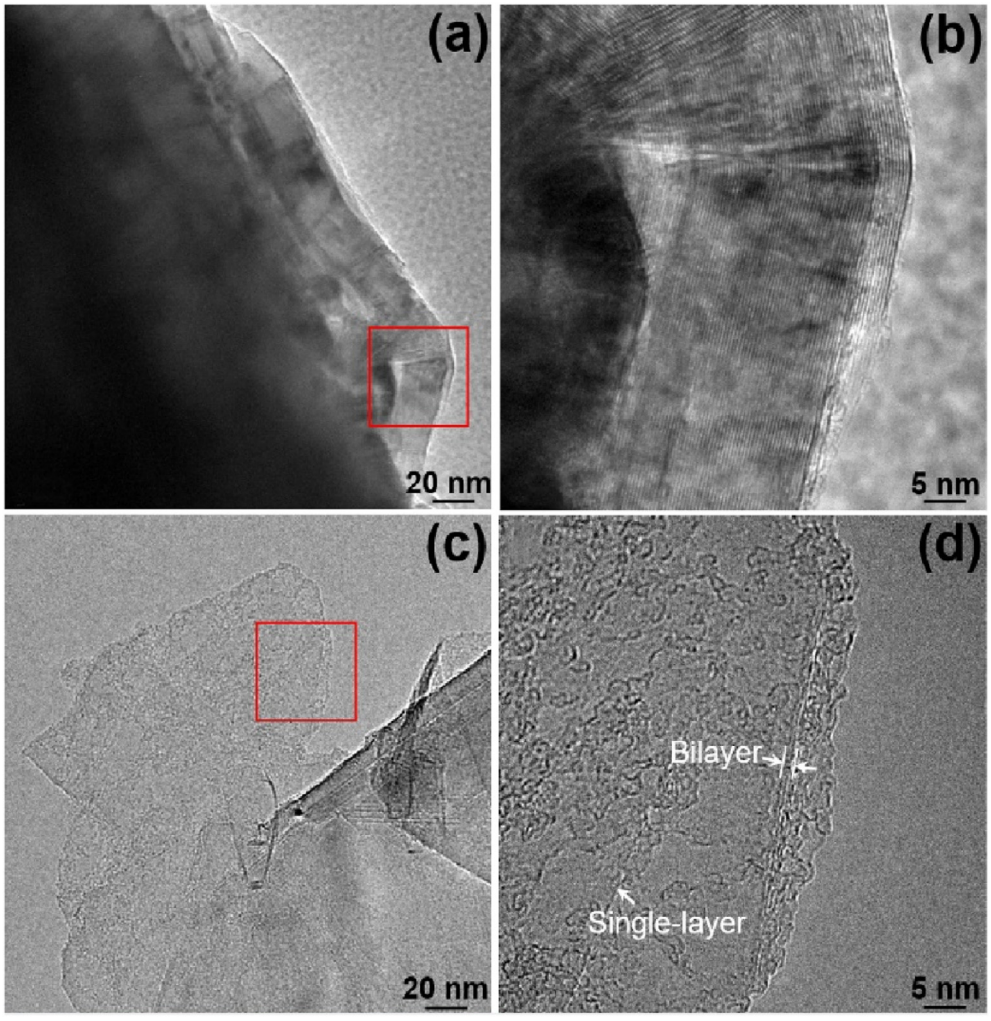

Fig. 5. TEM images of a) graphite, c) graphene produced by electron irradiation, b) high magnification of the area in a marked with a red rectangle; d) high magnification of the area in c marked with a red rectangle [105] (For interpretation of the references to color in this figure legend, the reader is referred to the Web version of this article).

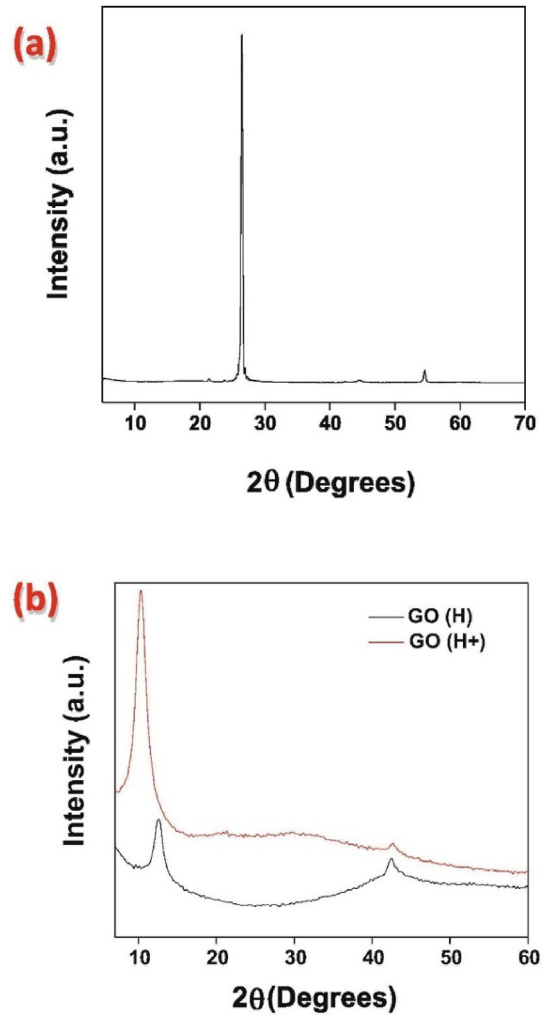

Fig. 6. XRD of (a) Graphite and (b) Graphene oxide (produced by Hummer's method). With the increasing amount of oxidizing agent (KMnO4), the peaks are shifted towards lower diffraction angles [37].

product should be treated with reducing agents before its application as graphene.

Although FTIR is a commonly used analytical technique capable of producing quick results, it is not suitable for the accurate measurement of the C/O ratio.

3.2. Raman spectroscopy

Raman spectroscopy is capable of identifying molecules with easily polarizable bonds. The numerous delocalized π electrons in the structure of graphite and graphene can be identified on a Raman spectrum as a characteristic peak at 1330–1350 cm^{-1} and an additional peak at 1580–1600 cm^{-1} (Fig. 2). Considering that graphene production from GO by reduction requires the reformation of the sp^2 structure of the carbon layer that had been broken by oxidation, this characteristic peak can be an indirect indicator of whether the reduction process was successful. However, the sp^2 structure cannot be restored in every case just by removing oxygen-containing functional groups from GO [60,64,66,70,74,75,77,80,81,85,86,90,94,96,99,104,106–109,112,114–119,122,124–126]. Although Raman spectroscopy is a quick and easy analytical tool requiring simple sample preparation, it shall not be used as a standalone technique since its findings need to be supported by other analytical tests.

3.3. UV-VIS spectroscopy

UV-VIS spectroscopy can reveal chromophore functional groups (i.e. molecular parts containing easily excitable non-bonding electron pairs). These include oxygen-containing functional groups. The measurement can be performed on liquid or gaseous samples. Therefore, graphene and GO must be dissolved in an appropriate solvent. UV-VIS spectra of graphene and GO usually show a peak associated with aromatic C–C bonds. This peak is near 230 nm for GO and 270 nm for graphene, as shown in Figs. 9b and 10. In most cases, a peak associated with C=O bonds is also observed at ~300 nm in GO samples [35,37,88,89,111,117,119,127–130]. Fig. 9a illustrates the difference in the visible range. The different colors of rGO and GO at the same concentration can be seen. Although the method shows a clear distinction between rGO and GO, it is not suitable for determining the C/O ratio of GO samples.

3.4. X-ray photoelectron spectroscopy (XPS)

When a sample is irradiated with X-rays, electrons are released from the material. The energy of the released electrons is characteristic of their original bonding state. Thus, the presence, absence, and even concentration of different oxygen-containing functional groups can be inferred in graphene and GO samples. C/O ratio can be determined by this method, and thus samples with different oxygen contents can be compared. In addition, the ratio of different oxygen-containing functional groups can be determined with XPS. Covalent bonds of carbon normally appear as broad peaks in the

Table 1
Characteristic peaks on the FTIR spectra of GO samples.

Vibration	Peak [cm^{-1}]	References
O–H stretching	3200–3500	[52,88,90,100,107–109,111,116,119]
O–H bending	1350–1650	[78,79,88,89,98,99,108,109,119]
C=O stretching	1590–1750	[34,52,78,79,88–90,97–101,106–111,116,119,120]
C–OH stretching	1220–1410	[52,90,100,106,109,111,116,119,121]
C–O stretching	1040–1100[a]	[34,52,78,88,90,97,100,106,107,109,116,119]
C–O stretching	1200–1270[b]	[34,39,90,109,121–123]
C–O stretching	1350–1430[c]	[39,85,107,111]
C–O–C stretching	950–1250	[74,79,85,89,97,98,106–109,111,113,116,119,121,123]
C=C stretching	1550–1630	[34,39,74,78–80,85,88–90,97,98,106–108,113,116,123]
–CH2–stretching	2850–2980	[39,89,90,108]

[a] Hydroxyl groups.
[b] Epoxy groups.
[c] Carboxyl groups.

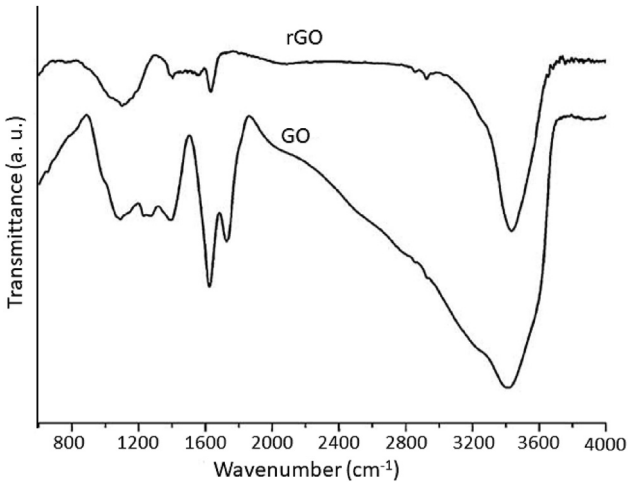

Fig. 7. FTIR spectra of GO and rGO [52].

300–280 eV binding energy range. C–C bonds have a binding energy of 284.8 eV. Oxidized functional groups are shifted to higher binding energies: 285.8 eV for C–N, 286.7 eV for C–O, 287.7 eV for C=O, and 288.7 eV for O–C=O groups [34,52,60,70,79–82,90,91,93,102,107–109,111,112,115–119,121,122,124-142]. A disadvantage of XPS is that information is gathered only from the surface of the sample due to the short free path of the exiting electrons. Therefore, it is mainly suitable for examining coatings and thin layers.

In Fig. 11, XPS spectra of GO samples prepared with different reaction times are shown. It can be seen that the peak areas increase with increased reaction times and hence oxidation rates. Fig. 11b and d also illustrate how individual peaks merge and yield the final spectrum [75].

To ensure successful measurement, special care has to be taken to avoid contamination during sample preparation. An advantage of XPS is that it is suitable for testing pure graphene or GO samples as well as their composites with elastomers. Thus, in-situ GO reduction can be evaluated.

3.5. Energy dispersive spectroscopy (EDS)

EDS is typically used as part of SEM examination; this way, morphological information is also gathered. On the spectrum, the intensity (relative number) of the photons leaving the samples due to excitation are represented as a function of their energy. The peaks can be linked with the atoms present in the sample (atomic numbers from boron to uranium); thus, the C/O ratio of the sample can be easily determined [64,75,78,82,85,86, 88,92,95–97,99,103,107,109,113,129,133,138,142].

In addition to the C/O ratio, EDS can also be used to detect the presence of impurities (e.g. residues of oxidants) in the sample. Al-Gaashani et al. prepared GO samples by different methods and investigated them using EDS (Fig. 12) [113]. Before oxidation, the oxygen content of graphite was undetectable (Fig. 12a). The first sample (Fig. 12b) was exposed to a 70:20:10 mixture by weight of H_2SO_4, H_3PO_4, and HNO_3, the second sample (Fig. 12c) to a 90:10 mixture by weight of H_2SO_4 and H_3PO_4, and the third sample (Fig. 12c) was placed in an ultrasonic bath after acidic oxidation, during which some reduction occurred. Accordingly, the S peak from the H_2SO_4 is visible in Fig. 12b and c, while a smaller O peak due to reduction can be seen in Fig. 12d.

The main limitation of the EDS is that it is not possible to distinguish between functional groups. During the evaluation, it has to be considered which part of the sample has been analyzed. In some cases, it may be necessary to compare several areas to arrive at the correct conclusions. Morphological information from the SEM examination can help. Since only the top layer is examined, it is necessary to prepare and examine several specimens from various cross-sections of the samples. Considering these, EDS is suitable for the evaluation of the in-situ reduction of GO in

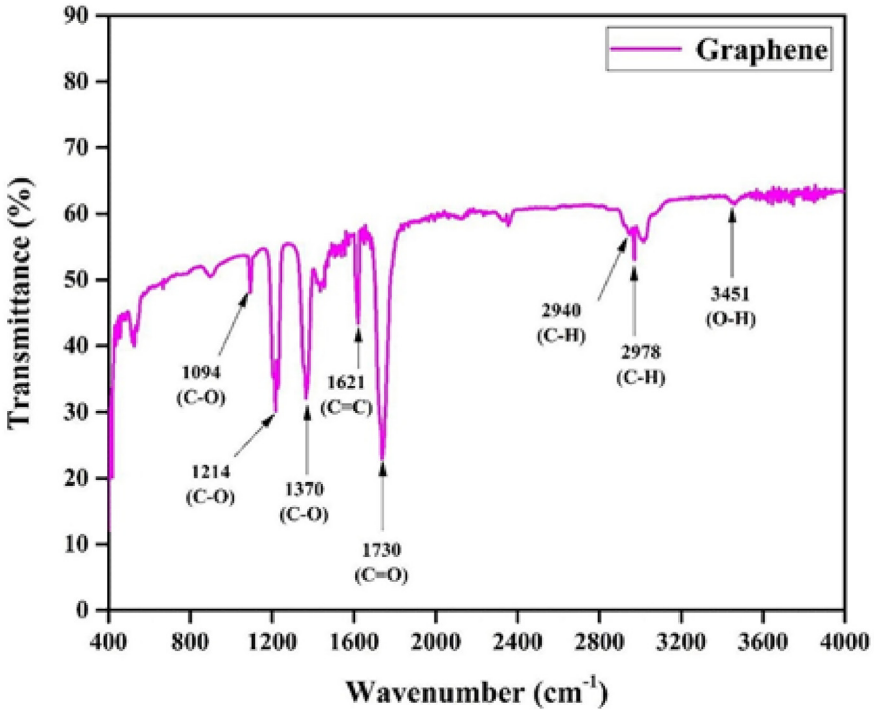

Fig. 8. FTIR spectrum of a graphene sample produced via electrolysis [39].

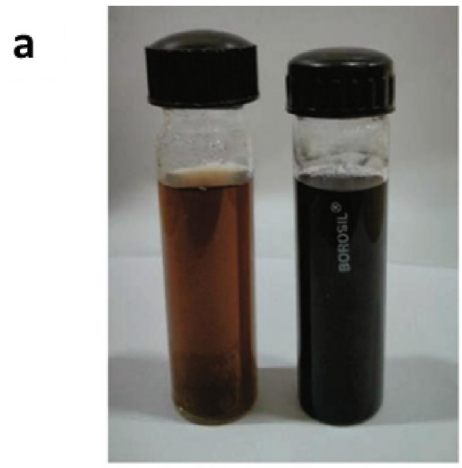

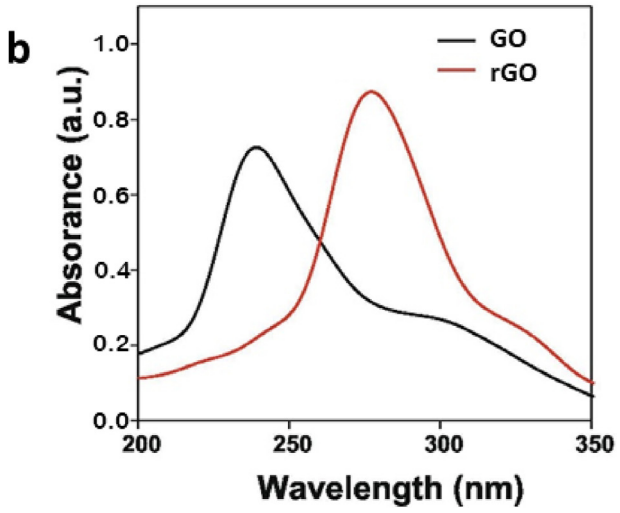

Fig. 9. a) GO on the left, rGO on the right b) UV spectra of the two materials [37].

elastomer composites. EDS is an excellent tool for determining the C/O ratio in GO and graphene samples. However, it has to be combined with other methods to obtain information about the types of functional groups present.

3.6. X-ray diffraction (XRD)

XRD shows a clear difference between graphite, graphene, and GO samples. Since XRD analyzes the crystallinity of samples, the oxygen content of GO or graphene can be inferred indirectly from XRD results. The XRD spectrum of graphite shows a single narrow peak corresponding to the spacing of the layers in graphite crystals (Fig. 13). During oxidation, oxygen-containing functional groups are incorporated, so the interlaminar spacing increases. Considering the random appearance of these functional groups, the interlaminar space is not uniform. For this reason, the peak on the spectrum of GO shifted to the left and broadened, compared to graphite's [34,52,60,70,74,79,81,85,86,89,94,96,98,99,101,102,104,108–112,114,120,122,129,131,132,134,135,140,141,143,144]. XRD is not suitable for distinguishing between different oxygen-containing functional groups or determining their concentration; consequently, the C/O ratio cannot be accurately quantified. However, this method may be suitable for indirectly monitoring the efficiency of

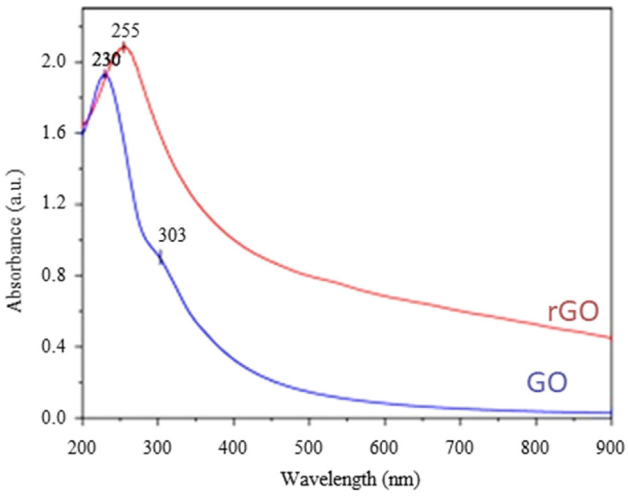

Fig. 10. UV-VIS spectra of rGO and GO [128].

oxidation since all adjacent layers must be separated during oxidation, which is indicated by the disappearance of the peak at 26.5°.

4. Preparation of graphene-rubber nanocomposites

Due to the size of graphene, graphene-containing composites are classified as nanocomposites. The properties of these materials are determined by their morphology and structure. The formation of the morphology primarily depends on the mixing technology used. The advantage of nanocomposites is the size effect, which implies that the reinforcing particles contain fewer defects than their larger counterparts. Thus, they can improve the mechanical properties of polymers to a greater extent. Nevertheless, this effect is only achieved if the nanoparticles are homogeneously dispersed in the matrix. Otherwise, nanoparticles form aggregates that are more prone to defects, and hence the mechanical properties of the composite are compromised [136,137,145,146].

Traditionally, the production of polymer nanocomposites follows three distinct strategies. Nanoparticles can be dispersed in the matrix by mixing methods known in polymer technology (i.e. extrusion or internal mixing). Suppose there is a solvent available in which both the polymer and the nanoparticle are soluble. In that case, the composite can be prepared by mixing the two solutions and then removing the solvent. The third way is in-situ polymerization. In this case, the nanoparticles are dispersed in the monomer or oligomer, followed by the polymerization process [147]. In the case of graphene/elastomer nanocomposites, the possible processes are similar but not identical. The relevant methods used for elastomer nanocomposites are discussed in this chapter.

4.1. Melt mixing

Melt mixing is similar to the first strategy described above. Similarly to extrusion, nanoparticles are directly mixed into the uncured rubber matrix, and then the mixture is vulcanized. Melt mixing is typically performed on a rolling mill or in an internal mixer. The main advantage of this process is its adaptability to current technology, as necessary equipment is used in rubber processing plants anyway to ensure the dispersion of other additives. If the elastomer is available in block form, melt mixing is the simplest mixing process to apply. However, a significant drawback of this method is the formation of

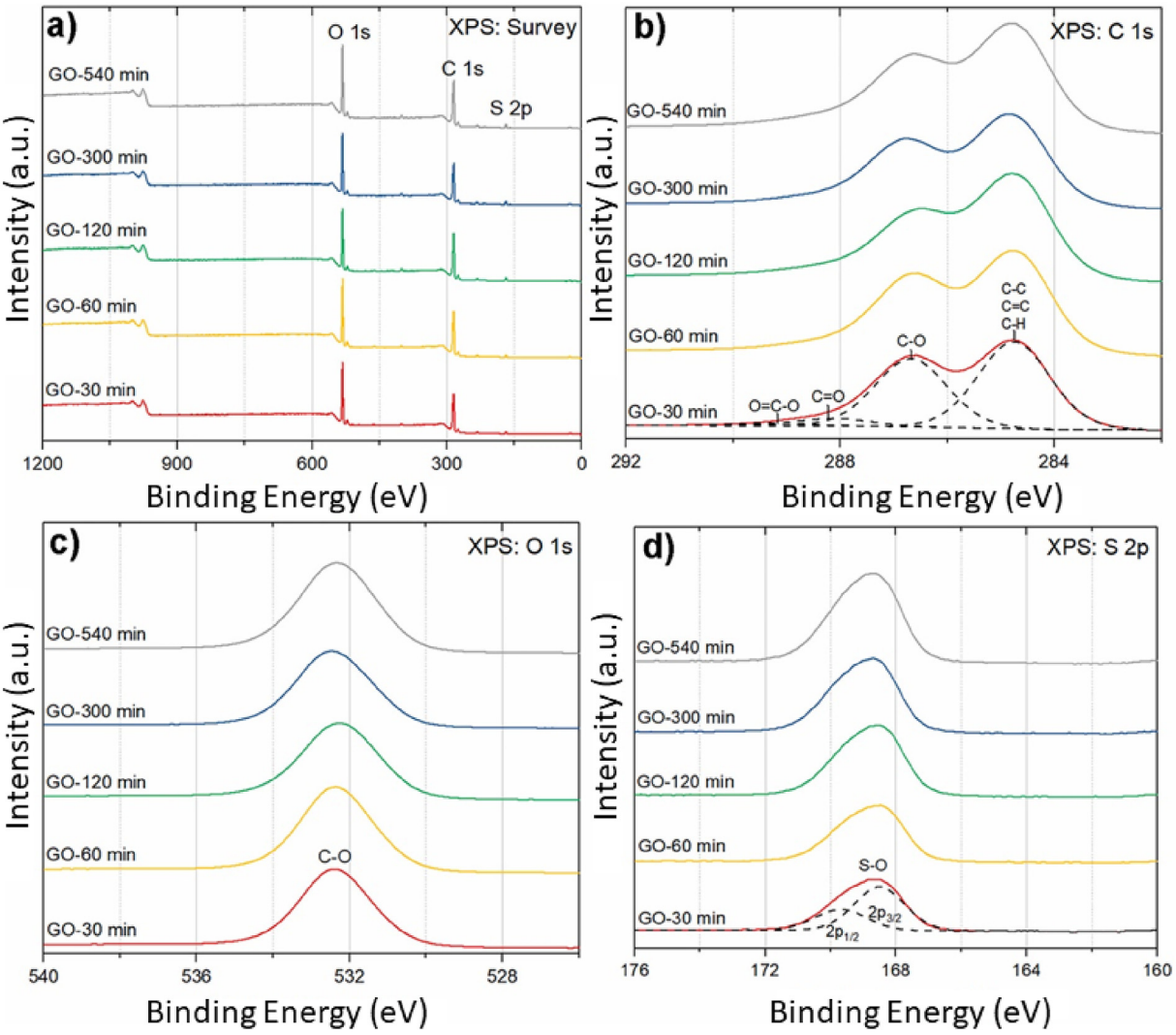

Fig. 11. XPS spectra of the GOs prepared with different reaction times. a) Complete spectra; High-resolution spectra of b) C 1s, c) O 1s and d) S 2p. Deconvolution was performed for all spectra but is shown only for the 30-min lines [75].

agglomerates since traditional mixing techniques cannot provide enough shearing to separate graphene layers from each other [41,63,90,100,110,118,120,127,139–141,148,149] . The dispersion can be facilitated by compatibilizers or surface treatment of nanoparticles. Thereby stronger interactions with the matrix are formed [142,143,150,151].

4.2. Solution mixing

Solution mixing is the direct adaptation of the second strategy described above. Graphene must be available dispersed in an organic solvent that readily dissolves the base rubber polymer. A rubber solution must also be prepared, and nanoparticles can be dispersed in the polymer when the two solutions are mixed, followed by solvent removal and vulcanization. To achieve proper dispersion, surface treatment of nanoparticles may be necessary. Mixing may be aided with ultrasound to avoid aggregation. Altogether, solution mixing is relatively fast yet quite challenging to incorporate into traditional rubber compounding [148]. It can be an obvious choice if the elastomer was produced via solvent polymerization and the graphene was produced via solvent intercalation. Solution mixing can yield a 3D segregated graphene network structure, meaning that the graphene particles are interconnected in the nanocomposite. This network can contribute to specific nanocomposite properties, such as enhanced electrical conductivity or reduced vapor permeability, compared to samples prepared via melt mixing [152]. The most considerable disadvantage of solution mixing is the use of organic solvents, which is expensive to recover and requires great environmental care [34,63,91,101,106,116,141,145,146,153,154].

4.3. Latex mixing

Latex mixing is a subset of solution mixing. In this case, the solvent used for the process is water. During latex mixing, the aqueous dispersion of nanoparticles is mixed into rubber latex. This is followed by coagulation, drying, compounding with other additives, and vulcanization [148]. Latex mixing may be useful for products made of natural rubber (NR) or emulsion-type rubber polymers, where the matrix material is obtained in the form of latex. It may also be preferable if the graphene is produced in aqueous dispersion and available in this form. Advantages of latex mixing include the achievable high degree of dispersion, the simplicity of the process, and its low cost. If additives are added before removing the water, further agglomeration can be prevented, and thus a 3D segregated graphene network can be formed, similarly to the case of solution mixing [58,147,148,155]. Also, in

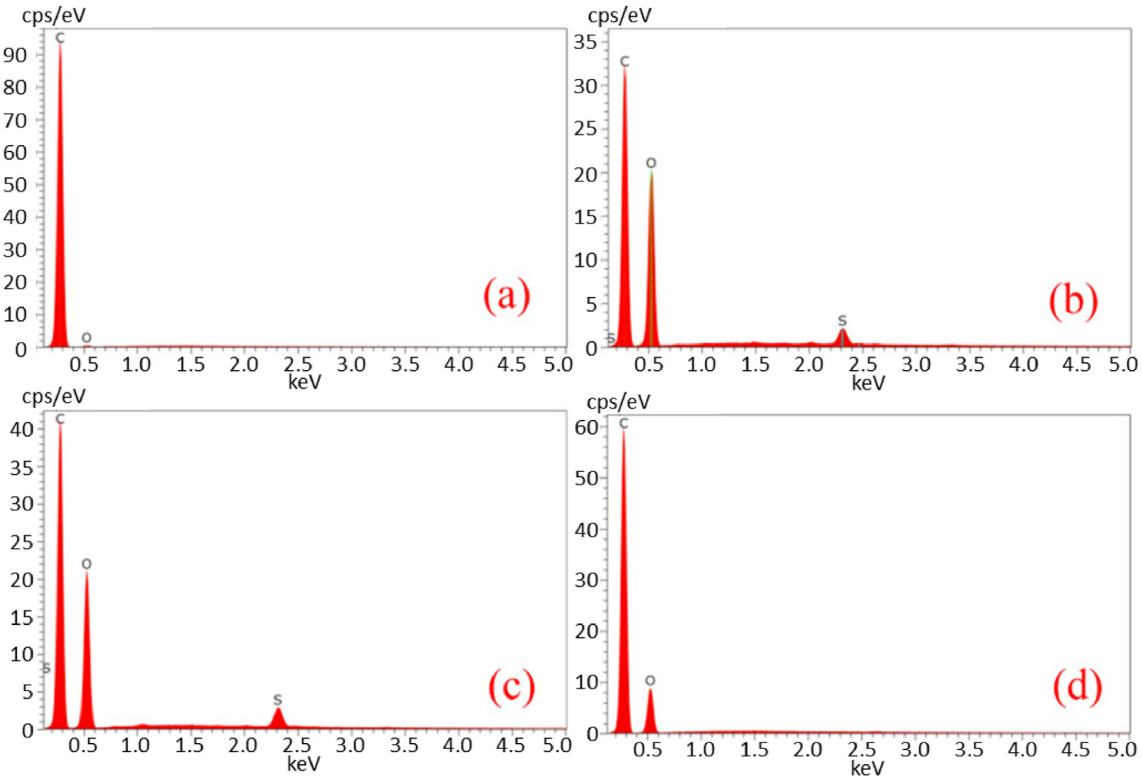

Fig. 12. EDS results: a) graphite; b) GO prepared with a 70:20:10 mixture of sulfuric acid, phosphoric acid, and nitric acid; c) GO prepared with a 90:10 mixture of sulfuric and phosphoric acid; d) ultrasonically reduced GO [113].

case of latex mixing, no organic solvent is required, making latex mixing an environmentally friendly option. However, a disadvantage is that high particle concentrations cannot be achieved in aqueous dispersions of nanoparticles, resulting in high water demand and an immense need for drying. In addition, the dispersion of nanoparticles is an energy-intensive process, often performed using ultrasound, making scalability difficult [148]. Latex mixing may be used not only for graphene but also for GO and rGO, as most oxidation-reduction pathways take part in an aqueous phase. Several examples of the use of latex mixing to produce graphene/elastomer composites are reported in literature [52,57,60,63,78,87–89,92,97–99,102,106,107,109,114,116,124,133, 141,149,156].

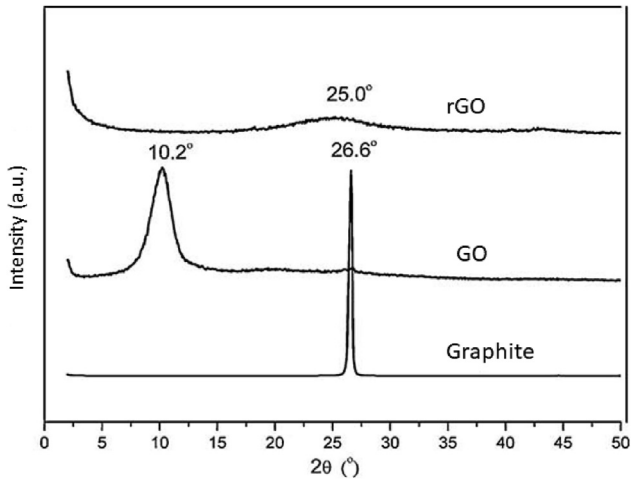

Fig. 13. XRD spectra of graphite, GO, and rGO [52].

4.4. In-situ polymerization

In-situ polymerization starts from monomers or oligomers, which chemically react with each other in the mold to form polymer chains and cross-linkages. The starting monomer or oligomer is typically in liquid form, so additives (even nanoparticles) can be easily dispersed in it. In-situ polymerization is a common process for creating thermoset products. For the majority of elastomers, in-situ polymerization is not applicable, as the blend preparation starts from polymer. An exception to this is polyurethane elastomers (PUR). Polyurethanes are a large family of materials with a wide range of properties and are therefore used in many different applications. Additives are added to the mold by mixing them with the diisocyanate or diol (monomers of PUR). In the case of nanoparticles, dispersion in liquid is easier to achieve than in a polymer melt. Although mixing helped by ultrasonication may be needed for preventing the aggregation of the nanoparticles. However, when adding GO, it must be taken into account that the hydroxyl groups on the GO nanoparticles can react with the isocyanate groups in the same way as the hydroxyl groups on the diol. Although in-situ polymerization is not applicable for most elastomers, it is the most obvious way to disperse the nanoparticles in PUR products [150–163].

5. Testing methods for nanoparticle distribution in the composite

5.1. Scanning electron microscopy (SEM)

SEM is widely used to investigate the morphology of polymer composites, so its application is obvious for composites containing graphene or GO. The images can show the arrangement of particles in the matrix, so the level of dispersion may be determined. This is particularly important because the aggregation of particles impairs

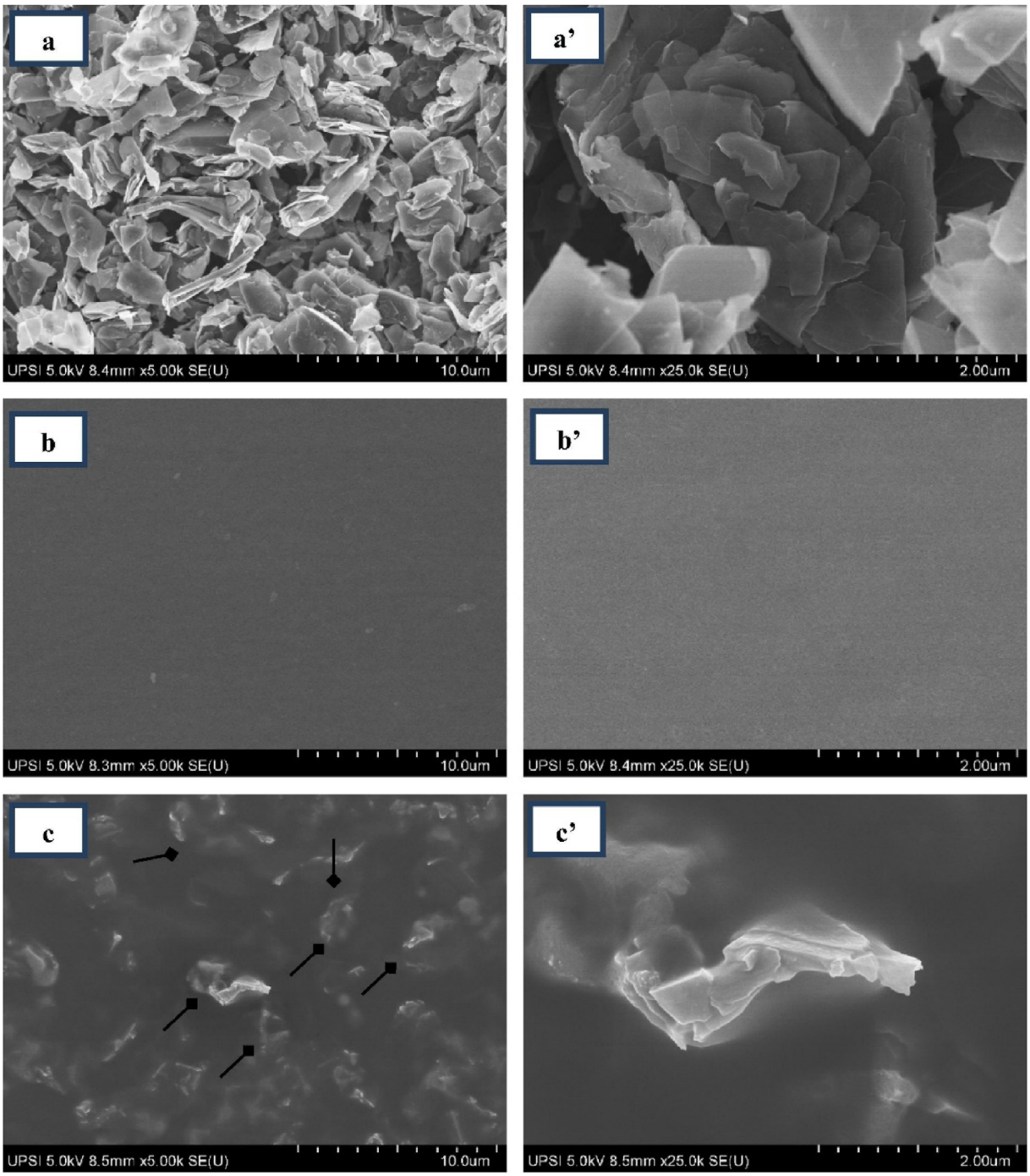

Fig. 14. SEM images, a-a′) graphene particles, b-b′) NR, c-c′) graphene particles in NR matrix [170].

the mechanical properties of the composite [6,78,80,88,90,92,97,99,102,106,107,109,111,116,121,140,149,150,157–162,164–169]. The method can be beneficial when the percolation of graphene particles is desired (typically in electrically conductive composites).

Fig. 14 contains SEM images of graphene/NR nanocomposites. Images of these composites reveal the degree of aggregation and show the interface between graphene and the rubber matrix [170].

5.2. Transmission electron microscopy (TEM)

TEM imaging provides an insight into the morphology of nanocomposites at a higher resolution than SEM. TEM images clearly show the size and arrangement of graphene or GO particles in the matrix. Conclusions can be drawn about the particle-matrix interaction, which determines the mechanical properties of the composite [41,52,60,89,99,106,107,109,114,116,117,124,133,140,149,160,167]. Because of the sheet-like shape of the particles, their orientation has to be considered during sample preparation. Only a narrow cross-section of the sample is visible in TEM images, so several specimens must be prepared from different angles to investigate a nanocomposite sample thoroughly.

Fig. 15 show TEM images of a GO/SBR (styrene-butadiene rubber) nanocomposite. The distribution of GO particles was successful; there is no sign of aggregates in the composite. Consequently,

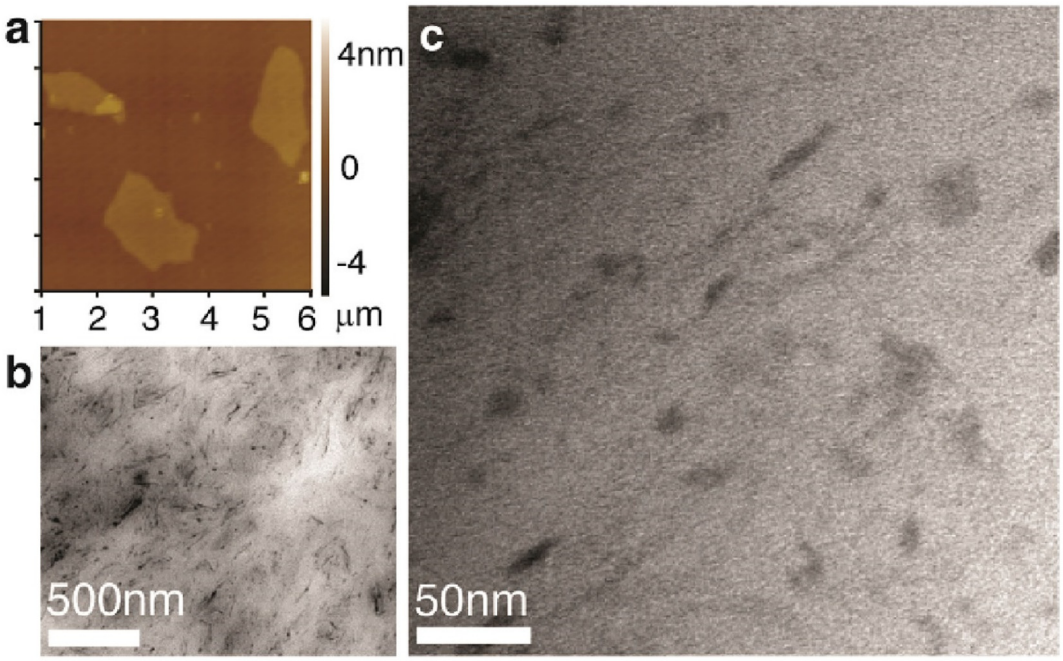

Fig. 15. a) AFM image of GO particles b-c) TEM images of GO/SBR composite, containing 7 phr GO [171].

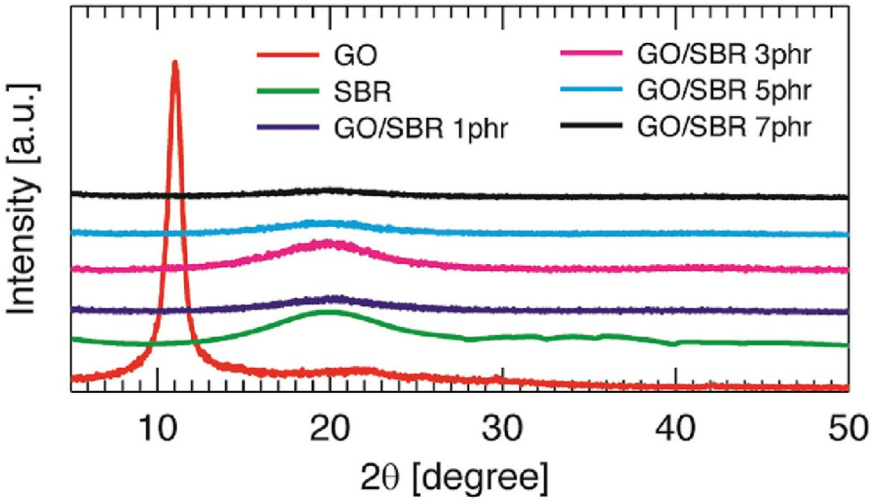

Fig. 16. XRD spectra of GO/SBR composites with different amounts of GO [171].

the mixing technology used (latex mixing in this case) is proven effective [171].

5.3. X-ray diffraction

Composites containing graphene or GO particles can be analyzed by XRD as well. The characteristic peak of graphite is a good indicator of the distance between graphene layers. However, the matrix's characteristic peaks can completely alter the spectrum. Therefore, the XRD spectrum of the pure matrix has to be compared to the spectrum of the composite to draw correct conclusions [41,78,88,97,106,107,116,124,133,161,165,168,172].

Fig. 16 shows the XRD spectra of GO/SBR composites with different GO contents. In the case of pure GO, one characteristic peak can be seen, indicating the spacing between layers. Due to the interlayer functional groups, its angle is lower than for graphite. This peak does not appear in the spectra of composites, indicating that complete exfoliation was achieved during mixing. The broad peak of SBR around 20° also appears in the spectra of the composites. This draws attention to the fact that the spectra of composites carry the characteristics of the individual components, yet are not suitable for quantitative analysis [171].

6. Conclusions

Graphene-based elastomer nanocomposites comprise an emerging field of materials science. They are expected to be employed in several industries for their beneficial properties. Graphene has the largest Young's modulus of all known materials, and as such, it has an exceptional potential in creating lightweight,

strongly reinforced nanocomposites. Due to its electrically conductive properties, it can play a role in electronics or even in electric cars in the future. Considering the sheer production volume of rubber tires, the ultimate goal would be to use graphene to increase their longevity and potentially decrease their rolling resistance. However, to achieve these goals, the quality of graphene and its homogeneous dispersion in the rubber matrix must be ensured.

Some of the preparation methods of graphene include the oxidation of graphite, as oxygen-containing functional groups increase the separation of layers. Consequently, two of the most important properties of graphene are its layer thickness and oxygen content. Graphene's reinforcing capabilities can be exploited to the fullest if it has the largest interface with the matrix, which can be achieved with the lowest possible layer thickness. Functionalization can change the quality of the graphene-polymer interaction. Higher oxygen content may be beneficial when combined with polar polymer matrices. However, most rubbers are non-polar, so high oxygen contents are generally undesirable.

As graphene nanocomposites comprise a relatively new research topic, there are no standardized tests for the accurate measurement of their properties. In this review, we evaluated several analytical techniques based on their applicability to the study of graphene and graphene-based nanocomposites. We concluded that most spectroscopic tools could only qualitatively measure specific properties. However, quantitative analysis is also possible. X-ray diffraction can be used to simultaneously gain information about the layer thickness and the oxygen content of graphene. It is also suitable for determining whether graphene is uniformly dispersed in the rubber matrix. These findings must be validated by Raman spectroscopy, transmission electron microscopy, and energy dispersive spectroscopy.

Declaration of competing interest

The authors declare that they have no known competing financial interests or personal relationships that could have appeared to influence the work reported in this paper.

Data availability

No data was used for the research described in the article.

Acknowledgments

The research reported in this paper and carried out at BME has been supported by the National Research, Development and Innovation Office, Hungary (2017-2.3.6-TÉT-CN-2018-00002). The research reported in this paper is part of project no. BME-NVA-02, implemented with the support provided by the Ministry of Innovation and Technology of Hungary from the National Research, Development and Innovation Fund, financed under the TKP2021 funding scheme.

References

[1] K.S. Novoselov, A.K. Geim, S.V. Morozov, D. Jiang, Y. Zhang, S.V. Dubonos, I.V. Grigorieva, A.A. Firsov, Electric field effect in atomically thin carbon films, Science 306 (2004) 666–669, https://doi.org/10.1126/science.1102896.

[2] Q. Zhou, J. Zheng, S. Onishi, M.F. Crommie, A.K. Zettl, Graphene electrostatic microphone and ultrasonic radio, Proc. Natl. Acad. Sci. USA 112 (2015) 8942–8946, https://doi.org/10.1073/pnas.1505800112.

[3] Z. Peng, R. Ye, J.A. Mann, D. Zakhidov, Y. Li, P.R. Smalley, J. Lin, J.M. Tour, Flexible boron-doped laser-induced graphene microsupercapacitors, ACS Nano 9 (2015) 5868–5875, https://doi.org/10.1021/acsnano.5b00436.

[4] M.F. El-Kady, M. Ihns, M. Li, J.Y. Hwang, M.F. Mousavi, L. Chaney, A.T. Lech, R.B. Kaner, Engineering three-dimensional hybrid supercapacitors and microsupercapacitors for high-performance integrated energy storage, Proc. Natl. Acad. Sci. USA. 112 (2015) 4233–4238, https://doi.org/10.1073/pnas.1420398112.

[5] R. Narayanan, H. Yamada, M. Karakaya, R. Podila, A.M. Rao, P.R. Bandaru, Modulation of the electrostatic and quantum capacitances of few layered graphenes through plasma processing, Nano Lett. 15 (2015) 3067–3072, https://doi.org/10.1021/acs.nanolett.5b00055.

[6] D. Niu, W. Jiang, G. Ye, K. Wang, L. Yin, Y. Shi, B. Chen, F. Luo, H. Liu, Graphene-elastomer nanocomposites based flexible piezoresistive sensors for strain and pressure detection, Mater. Res. Bull. 102 (2018) 92–99, https://doi.org/10.1016/j.materresbull.2018.02.005.

[7] S. Tkachev, M. Monteiro, J. Santos, E. Placidi, M.B. Hassine, P. Marques, P. Ferreira, P. Alpuim, A. Capasso, Environmentally friendly graphene inks for touch screen sensors, Adv. Funct. Mater. 31 (2021), 2103287, https://doi.org/10.1002/adfm.202103287.

[8] S. Kanakia, J.D. Toussaint, S.M. Chowdhury, G. Lalwanim, T. Tembulkar, T. Button, K.R. Shroyer, W. Moore, B. Sitharaman, Physicochemical characterization of a novel graphene-based magnetic resonance imaging contrast agent, Int. J. Nanomed. 8 (2013) 2821–2833, https://doi.org/10.2147/IJN.S47062.

[9] Z. Tehrani, G. Burwell, M.A. Mohd Azmi, A. Castaing, R. Rickman, J. Almarashi, P. Dunstan, A. Miran Beigi, S.H. Doak, O.J. Guy, Generic epitaxial graphene biosensors for ultrasensitive detection of cancer risk biomarker, 2D Mater. 1 (2014), https://doi.org/10.1088/2053-1583/1/2/025004.

[10] T.R. Nayak, H. Andersen, V.S. Makam, C. Khaw, S. Bae, X. Xu, R. Ee P.-L, J.-H. Ahn, B.H. Hong, G. Pastorin, B. Özyilmaz, Graphene for controlled and accelerated osteogenic differentiation of human mesenchymal stem cells, ACS Nano 5 (2011) 4670–4678, https://doi.org/10.1021/nn200500h.

[11] D.-W. Park, A.A. Schendel, S. Mikael, S.K. Brodnick, T.J. Richner, J.P. Ness, M.R. Hayat, F. Atry, S.T. Frye, R. Pashaie, S. Thongpang, Z. Ma, J.C. Williams, Graphene-based carbon-layered electrode array technology for neural imaging and optogenetic applications, Nat. Commun. 5 (2014), https://doi.org/10.1038/ncomms6258.

[12] T. Jiang, W. Sun, Q. Zhu, N.A. Burns, S.A. Khan, R. Mo, Z. Gu, Furin-mediated sequential delivery of anticancer cytokine and small-molecule drug shuttled by graphene, Adv. Mater. 27 (2015) 1021–1028, https://doi.org/10.1002/adma.201404498.

[13] J.-r. Hou, S.-s. Huang, N. Zhang, D.-y. Liu, Z.-j. Zhang, H.-s. Yang, L. Zong, Y.-x. Duan, J.-m. Zhang, Reinforcing natural rubber by amphiphilic graphene oxide for high-performance catheters, Polymer 232 (2021), https://doi.org/10.1016/j.polymer.2021.124142.

[14] Z. Lin, Z. Wang, X. Zhang, D. Diao, Superhydrophobic, photo-sterilize, and reusable mask based on graphene nanosheet-embedded carbon (GNEC) film, Nano Res. 14 (2021) 1110–1115, https://doi.org/10.1007/s12274-020-3158-1.

[15] S.M. Holmes, P. Balakrishnan, V.S. Kalangi, X. Zhang, M. Lozada-Hidalgo, P.M. Ajayan, R.R. Nair, 2D crystals significantly enhance the performance of a working fuel cell, Adv. Energy Mater. 7 (2017), https://doi.org/10.1002/aenm.201601216.

[16] J.T.-W. Wang, J.M. Ball, E.M. Barea, A. Abate, J.A. Alexander-Webber, J. Huang, M. Saliba, I. Mora-Sero, J. Bisquert, H.J. Snaith, R.J. Nicholas, Low-temperature processed electron collection layers of graphene/TiO_2 nanocomposites in thin film perovskite solar cells, Nano Lett. 14 (2014) 724–730, https://doi.org/10.1021/nl403997a.

[17] Y. Song, X. Li, C. Mackin, X. Zhang, W. Fang, T. Palacios, H. Zhu, J. Kong, Role of interfacial oxide in high-efficiency graphene-silicon Schottky barrier solar cells, Nano Lett. 15 (2015) 2104–2110, https://doi.org/10.1021/nl505011f.

[18] X. Li, D. Xie, H. Park, M. Zhu, T.H. Zeng, K. Wang, J. Wei, D. Wu, J. Kong, H. Zhu, Ion doping of graphene for high-efficiency heterojunction solar cells, Nanoscale 5 (2013) 1945–1948, https://doi.org/10.1039/C2NR33795A.

[19] X. Li, D. Xie, H. Park, T.H. Zeng, K. Wang, J. Wei, M. Zhong, D. Wu, J. Kong, H. Zhu, Anomalous behaviors of graphene transparent conductors in graphene–silicon heterojunction solar cells, Adv. Energy Mater. 3 (2013) 1029–1034, https://doi.org/10.1002/aenm.201300052.

[20] Y. Huang, R. Field, Q. Chen, Y. Peng, M.S. Walczak, H. Zhao, G. Zhu, Z. Liu, L. Li, Laser induced molybdenum sulphide loading on doped graphene cathode for highly stable lithium sulphur battery, Commun. Chem. 2 (2019) 138, https://doi.org/10.1038/s42004-019-0240-2.

[21] C. Xu, A. Cui, Y. Xu, X. Fu, Graphene oxide–TiO2 composite filtration membranes and their potential application for water purification, Carbon 62 (2013) 465–471, https://doi.org/10.1016/j.carbon.2013.06.035.

[22] X. Ge, G. Su, W. Che, J. Yang, X. Zhou, Z. Wang, Y. Qu, T. Yao, W. Liu, Y. Wu, Atomic filtration by graphene oxide membranes to access atomically dispersed single atom catalysts, ACS Catal. 10 (2020) 10468–10475, https://doi.org/10.1021/acscatal.0c02203.

[23] A. Mohammadi, M.R. Daymond, A. Docoslis, Graphene oxide membranes for isotopic water mixture filtration: preparation, physicochemical characterization, and performance assessment, ACS Appl. Mater. Interfaces 12 (2020) 34736–34745, https://doi.org/10.1021/acsami.0c04122.

[24] C.A. Ruiz-Torres, J. Kang, K.M. Kang, K.M. Cho, Y.T. Nam, C. Byon, Y.-Y. Chang, D.W. Kim, H.-T. Jung, Graphene-based ultrafast nanofiltration membrane under cross-flow operation: effect of high-flux and filtered solute on membrane performance, Carbon 185 (2021) 641–649, https://doi.org/10.1016/j.carbon.2021.09.060.

[25] V. Acar, S. Erden, M. Sarikanat, Y. Seki, H. Akbulut, M.O. Seydibeyoglu, Graphene oxide modified carbon fiber prepregs: a mechanical comparison of the

effects of oxidation methods, Express Polym. Lett. 14 (2020) 1106–1115, https://doi.org/10.3144/expresspolymlett.2020.90.
[26] M.C.F. da Costa, M.R.M. Souza, D.R.G. Larrude, G.J.M. Fechine, Adhesion between graphene and polymers: a surface analysis perspective, Express Polym. Lett. 13 (2019) 52–64, https://doi.org/10.3144/expresspolymlett.2019.6.
[27] I. Larraza, B. Alonso-Lerma, K. Gonzalez, N. Gabilondo, R. Perez-Jimenez, M.A. Corcuera, A. Arbelaiz, A. Eceiza, Waterborne polyurethane and graphene/graphene oxide-based nanocomposites: reinforcement and electrical conductivity, Express Polym. Lett. 14 (2020) 1018–1033, https://doi.org/10.3144/expresspolymlett.2020.83.
[28] H. Guo, P. Ji, I.Z. Halász, D.Z. Pirityi, T. Bárány, Z. Xu, L. Zheng, L. Zhang, L. Liu, S. Wen, Enhanced fatigue and durability properties of natural rubber composites reinforced with carbon nanotubes and graphene oxide, Materials 13 (2020), https://doi.org/10.3390/ma13245746.
[29] A.T. Lawal, Recent progress in graphene based polymer nanocomposites, Cogent Chem. 6 (2020), 1833476, https://doi.org/10.1080/23312009.2020.1833476.
[30] A.K. Geim, K.S. Novoselov, The rise of graphene, Nat. Mater. 6 (2007) 183–191, https://doi.org/10.1038/nmat1849.
[31] M.J. Allen, V.C. Tung, R.B. Kaner, Honeycomb carbon: a review of graphene, Chem. Rev. 110 (2010) 132–145, https://doi.org/10.1021/cr900070d.
[32] A. Ciesielski, P. Samorì, Graphene via sonication assisted liquid-phase exfoliation, Chem. Soc. Rev. 43 (2014) 381–398, https://doi.org/10.1039/C3CS60217F.
[33] A. Reina, X. Jia, J. Ho, D. Nezich, H. Son, V. Bulovic, M.S. Dresselhaus, J. Kong, Large area, few-layer graphene films on arbitrary substrates by chemical vapor deposition, Nano Lett. 9 (2009) 30–35, https://doi.org/10.1021/nl801827v.
[34] D. Tumnantong, S. Poompradub, P. Prasassarakich, Poly(methyl methacrylate)-graphene emulsion prepared via RAFT polymerization and the properties of NR/PMMA-graphene composites, Eur. Polym. J. 139 (2020), https://doi.org/10.1016/j.eurpolymj.2020.109983.
[35] D.C. Marcano, D.V. Kosynkin, J.M. Berlin, A. Sinitskii, Z. Sun, A. Slesarev, L.B. Alemany, W. Lu, J.M. Tour, Improved synthesis of graphene oxide, ACS Nano 4 (2010) 4806–4814, https://doi.org/10.1021/nn1006368.
[36] W.S. Hummers, R.E. Offeman, Preparation of graphitic oxide, J. Am. Chem. Soc. 80 (1958) 1339, https://doi.org/10.1021/ja01539a017.
[37] P. Tambe, Synthesis and characterization of acid treated reduced graphene oxide, Mater. Today Proc. 49 (2022) 1294–1297, https://doi.org/10.1016/j.matpr.2021.06.381.
[38] H.S. Hussein, H.H. Shaarawy, N.H. Hussien, E.A. kader, S.I. Hawash, Synthesis of nano graphene for saving energy in water desalination, Clean. Eng. Technol. 4 (2021), https://doi.org/10.1016/j.clet.2021.100162.
[39] A.D. Pingale, A. Owhal, A.S. Katarkar, S.U. Belgamwar, J.S. Rathore, Facile synthesis of graphene by ultrasonic-assisted electrochemical exfoliation of graphite, Mater. Today Proc. 44 (2021) 467–472, https://doi.org/10.1016/j.matpr.2020.10.045.
[40] S. Yamanaka, M. Takase, Y. Kuga, Production of single- and few-layer graphene from graphite, in: S. Kaneko, P. Mele, T. Endo, T. Tsuchiya, K. Tanaka, M. Yoshimura, D. Hui (Eds.), Carbon-Related Materials in Recognition of Nobel Lectures by Prof. Akira Suzuki in ICCE, vols. 91–101, Springer International Publishing, Cham, 2017.
[41] S. Araby, Q. Meng, L. Zhang, H. Kang, P. Majewski, Y. Tang, J. Ma, Electrically and thermally conductive elastomer/graphene nanocomposites by solution mixing, Polymer 55 (2014) 201–210, https://doi.org/10.1016/j.polymer.2013.11.032.
[42] B. Jiang, C. Li, The synthesis and the catalytic properties of graphene-based composite materials, in: S. Kaneko, P. Mele, T. Endo, T. Tsuchiya, K. Tanaka, M. Yoshimura, D. Hui (Eds.), Carbon-Related Materials – In Recognition of Nobel Lectures by Prof. Akira Suzuki in ICCE, vol. 1, Springer, New York, 2017, pp. 3–26.
[43] A. Bianco, H.-M. Cheng, T. Enoki, Y. Gogotsi, R.H. Hurt, N. Koratkar, T. Kyotani, M. Monthioux, C.R. Park, J.M.D. Tascon, J. Zhang, All in the graphene family – a recommended nomenclature for two-dimensional carbon materials, Carbon 65 (2013) 1–6, https://doi.org/10.1016/j.carbon.2013.08.038.
[44] ISO/TS 80004-13:2017: Nanotechnologies – Vocabulary – Part 13: Graphene and Related Two-Dimensional (2D) Materials, 2017.
[45] S. Saiwari, W.K. Dierkes, J.W.M. Noordermeer, Chapter 8 recycling of individual waste rubbers, in: J.K. Kim, P. Saha, S. Thomas, J.T. Haponiuk, M.K. Aswathi (Eds.), Rubber Recycling: Challenges and Developments, vol. 1, The Royal Society of Chemistry, London, 2019, pp. 186–232.
[46] V.A. Eremeyev, Size effect in nanomaterials, in: H. Altenbach, A. Öchsner (Eds.), Encyclopedia of Continuum Mechanics, vols. 2290–2291, Springer Berlin Heidelberg, Berlin, Heidelberg, 2020.
[47] A.J. Crosby, J.Y. Lee, Polymer nanocomposites: the 'nano' effect on mechanical properties, Polym. Rev. 47 (2007) 217–229, https://doi.org/10.1080/15583720701271278.
[48] S. Fu, Z. Sun, P. Huang, Y. Li, N. Hu, Some basic aspects of polymer nanocomposites: a critical review, Nano Materials Science 1 (2019) 2–30, https://doi.org/10.1016/j.nanoms.2019.02.006.
[49] M.A. Ashraf, W. Peng, Y. Zare, K.Y. Rhee, Effects of size and aggregation/agglomeration of nanoparticles on the interfacial/interphase properties and tensile strength of polymer nanocomposites, Nanoscale Res. Lett. 13 (2018) 214, https://doi.org/10.1186/s11671-018-2624-0.
[50] Y. Lin, Z. Zeng, J. Zhu, S. Chen, X. Yuan, L. Liu, Graphene nanosheets decorated with ZnO nanoparticles: facile synthesis and promising application for enhancing the mechanical and gas barrier properties of rubber nanocomposites, RSC Adv. 5 (2015) 57771–57780, https://doi.org/10.1039/C5RA07582C.
[51] Y. Mao, S. Wen, Y. Chen, F. Zhang, P. Panine, T.W. Chan, L. Zhang, Y. Liang, L. Liu, High performance graphene oxide based rubber composites, Sci. Rep. 3 (2013), https://doi.org/10.1038/srep02508.
[52] Y. Zhan, J. Wu, H. Xia, N. Yan, G. Fei, G. Yuan, Dispersion and exfoliation of graphene in rubber by an ultrasonically-assisted latex mixing and in situ reduction process, Macromol. Mater. Eng. 296 (2011) 590–602, https://doi.org/10.1002/mame.201000358.
[53] S. Schopp, R. Thomann, K.-F. Ratzsch, S. Kerling, V. Altstädt, R. Mülhaupt, Functionalized graphene and carbon materials as components of styrene butadiene rubber nanocomposites prepared by aqueous dispersion blending, Macromol. Mater. Eng. 299 (2013) 319–329, https://doi.org/10.1002/mame.201300127.
[54] D. Frasca, D. Schulze, V. Wachtendorf, B. Krafft, T. Rybak, B. Schartel, Multilayer graphene/carbon black/chlorine isobutyl isoprene rubber nanocomposites, Polymers 8 (2016), https://doi.org/10.3390/polym8030095.
[55] K.K. Sadasivuni, A. Saiter, N. Gautier, S. Thomas, Y. Grohens, Effect of molecular interactions on the performance of poly(isobutylene-co-isoprene)/graphene and clay nanocomposites, Colloid Polym. Sci. 291 (2013) 1729–1740, https://doi.org/10.1007/s00396-013-2908-y.
[56] L. Gan, S. Shang, C.W.M. Yuen, S.-x. Jiang, N.M. Luo, Facile preparation of graphene nanoribbon filled silicone rubber nanocomposite with improved thermal and mechanical properties, Compos. B Eng. 69 (2015) 237–242, https://doi.org/10.1016/j.compositesb.2014.10.019.
[57] A. Noël, J. Faucheu, J.-M. Chenal, J.-P. Viricelle, E. Bourgeat-Lami, Electrical and mechanical percolation in graphene-latex nanocomposites, Polymer 55 (2014) 5140–5145, https://doi.org/10.1016/j.polymer.2014.08.025.
[58] Y. Zhan, M. Lavorgna, G. Buonocore, H. Xia, Enhancing electrical conductivity of rubber composites by constructing interconnected network of self-assembled graphene with latex mixing, J. Mater. Chem. 22 (2012) 10464–10468, https://doi.org/10.1039/C2JM31293J.
[59] Y. Lin, S. Liu, J. Peng, L. Liu, Constructing a segregated graphene network in rubber composites towards improved electrically conductive and barrier properties, Compos. Sci. Technol. 131 (2016) 40–47, https://doi.org/10.1016/j.compscitech.2016.05.012.
[60] L.P. Lim, J.C. Juan, N.M. Huang, L.K. Goh, F.P. Leng, Y.Y. Loh, Enhanced tensile strength and thermal conductivity of natural rubber graphene composite properties via rubber-graphene interaction, Mater. Sci. Eng., B 246 (2019) 112–119, https://doi.org/10.1016/j.mseb.2019.06.004.
[61] J. Wang, K. Zhang, Z. Cheng, M. Lavorgna, H. Xia, Graphene/carbon black/natural rubber composites prepared by a wet compounding and latex mixing process, Plast. Rubber Compos. 47 (2018) 398–412, https://doi.org/10.1080/14658011.2018.1516435.
[62] Z. Xie, Y. Cai, Y. Zhan, Y. Meng, Y. Li, Q. Xie, H. Xia, Thermal insulating rubber foams embedded with segregated carbon nanotube networks for electromagnetic shielding applications, Chem. Eng. J. 435 (2022), 135118, https://doi.org/10.1016/j.cej.2022.135118.
[63] H. Zhang, W. Xing, H. Li, Z. Xie, G. Huang, J. Wu, Fundamental researches on graphene/rubber nanocomposites, Adv. Indus. Eng. Polymer Res. 2 (2019) 32–41, https://doi.org/10.1016/j.aiepr.2019.01.001.
[64] J. Wu, G. Huang, H. Li, S. Wu, Y. Liu, J. Zheng, Enhanced mechanical and gas barrier properties of rubber nanocomposites with surface functionalized graphene oxide at low content, Polymer 54 (2013) 1930–1937, https://doi.org/10.1016/j.polymer.2013.01.049.
[65] S.-T. Hsiao, C.-C.M. Ma, H.-W. Tien, W.-H. Liao, Y.-S. Wang, S.-M. Li, Y.-C. Huang, Using a non-covalent modification to prepare a high electromagnetic interference shielding performance graphene nanosheet/water-borne polyurethane composite, Carbon 60 (2013) 57–66, https://doi.org/10.1016/j.carbon.2013.03.056.
[66] Y. Zhan, J. Wang, K. Zhang, Y. Li, Y. Meng, N. Yan, W. Wei, F. Peng, H. Xia, Fabrication of a flexible electromagnetic interference shielding Fe3O4@reduced graphene oxide/natural rubber composite with segregated network, Chem. Eng. J. 344 (2018) 184–193, https://doi.org/10.1016/j.cej.2018.03.085.
[67] K. Chand, X. Zhang, Y. Chen, Recent progress in MXene and graphene based nanocomposites for microwave absorption and electromagnetic interference shielding, Arab. J. Chem. 15 (2022), 104143, https://doi.org/10.1016/j.arabjc.2022.104143.
[68] C.J. Shearer, A.D. Slattery, A.J. Stapleton, J.G. Shapter, C.T. Gibson, Accurate thickness measurement of graphene, Nanotechnology 27 (2016), 125704. 10.1088/0957-4484/27/12/125704.
[69] M. Pfaffeneder-Kmen, I.F. Casas, A. Naghilou, G. Trettenhahn, W. Kautek, A Multivariate Curve Resolution evaluation of an in-situ ATR-FTIR spectroscopy investigation of the electrochemical reduction of graphene oxide, Electrochim. Acta 255 (2017) 160–167, https://doi.org/10.1016/j.electacta.2017.09.124.
[70] K. Grajewska, M. Lieder, Functionalization of graphene oxide coatings with phosphorus atoms and their corrosion resistance in sodium chloride environment, Diam. Relat. Mater. 118 (2021), 108533, https://doi.org/10.1016/j.diamond.2021.108533.

[71] Y. Han, J.-H. Eom, J.-S. Jung, S.-G. Yoon, Unprecedented flexibility of in-situ layer-by-layer stacked graphene with ultralow sheet resistance, Nano Today 37 (2021), 101105, https://doi.org/10.1016/j.nantod.2021.101105.
[72] S. Al-Saadi, R.K.S. Raman, M.R. Anisur, S. Ahmed, J. Crosswell, M. Alnuwaiser, C. Panter, Graphene coating on a nickel-copper alloy (Monel 400) for microbial corrosion resistance: electrochemical and surface characterizations, Corr. Sci. 182 (2021), 109299, https://doi.org/10.1016/j.corsci.2021.109299.
[73] D. Graf, F. Molitor, K. Ensslin, C. Stampfer, A. Jungen, C. Hierold, L. Wirtz, Spatially resolved Raman spectroscopy of single- and few-layer graphene, Nano Lett. 7 (2007) 238–242, https://doi.org/10.1021/nl061702a.
[74] G.S. Papanai, I. Sharma, G. Kedawat, B.K. Gupta, Qualitative analysis of mechanically exfoliated MoS2 nanosheets using spectroscopic probes, J. Phys. Chem. C 123 (2019) 27264–27271, https://doi.org/10.1021/acs.jpcc.9b09191.
[75] J. Aixart, F. Díaz, J. Llorca, J. Rosell-Llompart, Increasing reaction time in Hummers' method towards well exfoliated graphene oxide of low oxidation degree, Ceram. Int. 47 (2021) 22130–22137, https://doi.org/10.1016/j.ceramint.2021.04.235.
[76] Y. Liu, M. Yang, Wang G. YuanboYang, X. Li, Raman signatures of defects-dependent vibration modes in boron doped monolayer to multilayer graphene, Optik 228 (2021), 166232, https://doi.org/10.1016/j.ijleo.2020.166232.
[77] H.J. Salavagione, P.S. Shuttleworth, J.P. Fernández-Blázquez, G.J. Ellis, M.A. Gómez-Fatou, Scalable graphene-based nanocomposite coatings for flexible and washable conductive textiles, Carbon 167 (2020) 495–503, https://doi.org/10.1016/j.carbon.2020.05.108.
[78] G.V. Bianco, A. Sacchetti, M. Grande, A. D'Orazio, P. Capezzuto, G. Bruno, Highly conductive and transparent graphene: synergy of covalent and non-covalent co-doping, Appl. Surf. Sci. 564 (2021), 150377, https://doi.org/10.1016/j.apsusc.2021.150377.
[79] F.C. Rufino, A.M. Pascon, L.C.J. Espindola, F.H. Cioldin, D.R.G. Larrudé, J.A. Diniz, Definition of CVD graphene micro ribbons with lithography and oxygen plasma ashing, Carbon Trends 4 (2021), https://doi.org/10.1016/j.cartre.2021.100056.
[80] S. Hong, M. Park, S. Kwon, J. Oh, S. Bong, B. Krishnakumar, S.-Y. Ju, Formation of graphene nanostructures using laser induced vaporization of entrapped water, Carbon 183 (2021) 84–92, https://doi.org/10.1016/j.carbon.2021.06.071.
[81] F. Farivar, P.L. Yap, K. Hassan, T.T. Tung, D.N.H. Tran, A.J. Pollard, D. Losic, Unlocking thermogravimetric analysis (TGA) in the fight against 'Fake graphene' materials, Carbon 179 (2021) 505–513, https://doi.org/10.1016/j.carbon.2021.04.064.
[82] D. Yoon, H. Moon, H. Cheong, J. Choi, J. Choi, B. Park, Variations in the Raman spectrum as a function of the number of graphene layers, J. Kor. Phys. Soc. 55 (2009) 1299–1303, https://doi.org/10.3938/jkps.55.1299.
[83] Y. Hao, Y. Wang, L. Wang, Z. Ni, Z. Wang, R. Wang, C.K. Koo, Z. Shen, J.T.L. Thong, Probing layer number and stacking order of few-layer graphene by Raman spectroscopy, Small 6 (2010) 195–200, https://doi.org/10.1002/smll.200901173.
[84] J. Lee, K.S. Novoselov, H.S. Shin, Interaction between metal and graphene: dependence on the layer number of graphene, ACS Nano 5 (2011) 608–612, https://doi.org/10.1021/nn103004c.
[85] A.E.F. Oliveira, G.B. Braga, C.R.T. Tarley, A.C. Pereira, Thermally reduced graphene oxide: synthesis, studies and characterization, J. Mater. Sci. 53 (2018) 12005–12015.
[86] A. Dobrowolski, J. Jagiełło, D. Czołak, T. Ciuk, Determining the number of graphene layers based on Raman response of the SiC substrate, Phys. E Low dimens. Syst. Nanostruct. 134 (2021), https://doi.org/10.1016/j.physe.2021.114853.
[87] V. Kumar, Lee D.-J. Monika, High-actuation displacement with high flexibility for silicone rubber and few layer graphene composites, Sens. Actuat. Phys. 309 (2020), 111956, https://doi.org/10.1016/j.sna.2020.111956.
[88] H. Berber, E. Ucar, U. Sahinturk, Synthesis and properties of waterborne few-layer graphene oxide/poly(MMA-co-BuA) nanocomposites by in situ emulsion polymerization, Colloids Surf. A Physicochem. Eng. Asp. 531 (2017) 56–66, https://doi.org/10.1016/j.colsurfa.2017.07.057.
[89] R. Al-Gaashani, Y. Zakaria, O.-S. Lee, J. Ponraj, V. Kochkodan, M.A. Atieh, Effects of preparation temperature on production of graphene oxide by novel chemical processing, Ceram. Int. 47 (2021) 10113–10122, https://doi.org/10.1016/j.ceramint.2020.12.159.
[90] H. Jeon, Y. Kim, W.-R. Yu, J.U. Lee, Exfoliated graphene/thermoplastic elastomer nanocomposites with improved wear properties for 3D printing, Compos. B Eng. 189 (2020), https://doi.org/10.1016/j.compositesb.2020.107912.
[91] W. Lee, G. Lim, S.H. Ko, Significant thermoelectric conversion efficiency enhancement of single layer graphene with substitutional silicon dopants, Nano Energy 87 (2021), https://doi.org/10.1016/j.nanoen.2021.106188.
[92] Q. Li, S. Li, Q. Liu, X. Liu, J. Shui, X. Kong, Iodine cation bridged graphene sheets with strengthened interface combination for electromagnetic wave absorption, Carbon 183 (2021) 100–107, https://doi.org/10.1016/j.carbon.2021.07.015.
[93] M.J. Mason, B.J. Coleman, S. Saha, M.M. Mustafa, M.J. Green, Graphene signatures: identifying graphite and graphene grades via radio frequency heating, Carbon 182 (2021) 564–570, https://doi.org/10.1016/j.carbon.2021.06.046.
[94] H. Kang, Y. Zhang, J. Li, S. Wang, Z. Chen, Y. Sui, S. Zhao, G. Yu, Synthesis of scalable adlayer-free monolayer graphene film on Cu80Ni20 foil, Mater. Lett. 303 (2021), 130505, https://doi.org/10.1016/j.matlet.2021.130505.
[95] Q.A. Khan, A. Shaur, T.A. Khan, Y.F. Joya, M.S. Awan, Characterization of reduced graphene oxide produced through a modified Hoffman method, Cogent Chemistry 3 (2017), 1298980, https://doi.org/10.1080/23312009.2017.1298980.
[96] S.N. Alam, N. Sharma, L. Kumar, Synthesis of graphene oxide (GO) by modified hummers method and its thermal reduction to obtain reduced graphene oxide (rGO), Graphene 6 (2017) 1–18, https://doi.org/10.4236/graphene.2017.61001.
[97] N. Cao, Y. Zhang, Study of reduced graphene oxide preparation by Hummers' method and related characterization, J. Nanomater. 2015 (2015), https://doi.org/10.1155/2015/168125.
[98] B. Thomas, H.J. Maria, G. George, S. Thomas, N.V. Unnikrishnan, K. Joseph, A novel green approach for the preparation of high performance nitrile butadiene rubber-pristine graphene nanocomposites, Compos. B Eng. 175 (2019), https://doi.org/10.1016/j.compositesb.2019.107174.
[99] G. George, S.B. Sisupal, T. Tomy, B.A. Pottammal, A. Kumaran, V. Suvekbala, R. Gopimohan, S. Sivaram, L. Ragupathy, Thermally conductive thin films derived from defect free graphene-natural rubber latex nanocomposite: preparation and properties, Carbon 119 (2017) 527–534, https://doi.org/10.1016/j.carbon.2017.04.068.
[100] K.P. Jibin, V. Prajitha, S. Thomas, Silica-graphene oxide reinforced rubber composites, Mater. Today Proc. 34 (2021) 502–505, https://doi.org/10.1016/j.matpr.2020.03.100.
[101] Y. Sun, L. Ma, Y. Song, A.D. Phule, L. Li, Z.X. Zhang, Efficient natural rubber latex foam coated by rGO modified high density polyethylene for oil-water separation and electromagnetic shielding performance, Eur. Polym. J. 147 (2021), https://doi.org/10.1016/j.eurpolymj.2021.110288.
[102] A. Gao, F. Zhao, F. Wang, G. Zhang, S. Zhao, J. Cui, Y. Yan, Highly conductive and light-weight acrylonitrile-butadiene-styrene copolymer/reduced graphene nanocomposites with segregated conductive structure, Compos. Appl. Sci. Manuf. 122 (2019) 1–7, https://doi.org/10.1016/j.compositesa.2019.04.019.
[103] F.G. Torres, O.P. Troncoso, L. Rodriguez, G.E. De-la-Torre, Sustainable synthesis, reduction and applications of graphene obtained from renewable resources, Sustain. Mater. Technol. 29 (2021), https://doi.org/10.1016/j.susmat.2021.e00310.
[104] M. Wojtoniszak, X. Chen, R.J. Kalenczuk, A. Wajda, J. Łapczuk, M. Kurzewski, M. Drozdzik, P.K. Chu, E. Borowiak-Palen, Synthesis, dispersion, and cytocompatibility of graphene oxide and reduced graphene oxide, Colloids Surf. B Biointerfaces 89 (2012) 79–85, https://doi.org/10.1016/j.colsurfb.2011.08.026.
[105] J. Lu, X. Sui, B. Yang, J. Chen, L. Cai, S. Zhou, W. Li, M. Jiang, S. Hao, Ultrafast in-situ transformation of graphite into graphene nanosheets by high current pulsed electron beam direct irradiation, Appl. Surf. Sci. 572 (2022), https://doi.org/10.1016/j.apsusc.2021.151498.
[106] C. Hontoria-Lucas, A.J. López-Peinado, J.d.D. López-González, M.L. Rojas-Cervantes, R.M. Martín-Aranda, Study of oxygen-containing groups in a series of graphite oxides: physical and chemical characterization, Carbon 33 (1995) 1585–1592, https://doi.org/10.1016/0008-6223(95)00120-3.
[107] M. Raef, M. Razzaghi-Kashani, The role of interface in gas barrier properties of styrene butadiene rubber-reduced graphene oxide composites, Polymer 182 (2019), https://doi.org/10.1016/j.polymer.2019.121816.
[108] M. Mauro, V. Cipolletti, M. Galimberti, P. Longo, G. Guerra, Chemically reduced graphite oxide with improved shape anisotropy, J. Phys. Chem. C 116 (2012) 24809–24813, https://doi.org/10.1021/jp307112k.
[109] V. Phetarporn, S. Loykulnant, C. Kongkaew, A. Seubsai, P. Prapainainar, Composite properties of graphene-based materials/natural rubber vulcanized using electron beam irradiation, Mater. Today Commun. 19 (2019) 413–424, https://doi.org/10.1016/j.mtcomm.2019.03.007.
[110] F. Zia, K.M. Zia, W. Aftab, S. Tabasum, Z.-i.-H. Nazli, M. Mohammadi, M. Zuber, Synthesis and characterization of graphene nanoplatelets-hydroxyethyl cellulose copolymer-based polyurethane bionanocomposite system, Int. J. Biol. Macromol. 165 (2020) 1889–1899, https://doi.org/10.1016/j.ijbiomac.2020.10.069.
[111] E. Aliyev, V. Filiz, M.M. Khan, Y.J. Lee, C. Abetz, V. Abetz, Structural characterization of graphene oxide: surface functional groups and fractionated oxidative debris, Nanomaterials 9 (2019) 1180, https://doi.org/10.3390/nano9081180.
[112] N. Sharma, V. Sharma, Y. Jain, M. Kumari, R. Gupta, S.K. Sharma, K. Sachdev, Synthesis and Characterization of Graphene Oxide (GO) and Reduced Graphene Oxide (rGO) for Gas Sensing Application, vol. 376, Macromolecular Symposia, 2017, https://doi.org/10.1002/masy.201700006.
[113] R. Al-Gaashani, A. Najjar, Y. Zakaria, S. Mansour, M.A. Atieh, XPS and structural studies of high quality graphene oxide and reduced graphene oxide prepared by different chemical oxidation methods, Ceram. Int. 45 (2019) 14439–14448, https://doi.org/10.1016/j.ceramint.2019.04.165.
[114] C. Pannu, U.B. Singh, S. Kumar, A. Tripathi, D. Kabiraj, D.K. Avasthi, Engineering the strain in graphene layers with Au decoration, Appl. Surf. Sci. 308 (2014) 193–198, https://doi.org/10.1016/j.apsusc.2014.04.133.
[115] M.-p. Jiang, J.-h. Zhang, Y.-h. Wang, I. Ahmad, X. Guo, L.-m. Cao, Y.-k. Chen, L. Gan, J. Huang, Covalent-bond-forming method to reinforce rubber with

cellulose nanocrystal based on the thiol-ene click reaction, Compos. Commun. 27 (2021), https://doi.org/10.1016/j.coco.2021.100865.
[116] Z. Yang, H. Liu, S. Wu, Z. Tang, B. Guo, L. Zhang, A green method for preparing conductive elastomer composites with interconnected graphene network via Pickering emulsion templating, Chem. Eng. J. 342 (2018) 112–119, https://doi.org/10.1016/j.cej.2018.02.079.
[117] B. Zhong, Z. Jia, H. Dong, Y. Luo, D. Jia, F. Liu, One-step approach to reduce and modify graphene oxide via vulcanization accelerator and its application for elastomer reinforcement, Chem. Eng. J. 317 (2017) 51–59, https://doi.org/10.1016/j.cej.2017.02.072.
[118] Z. Zhang, P. Chen, W. Nie, Y. Xu, Y. Zhou, Enhanced mechanical, thermal and solvent resistance of silicone rubber reinforced by organosilica nanoparticles modified graphene oxide, Polymer 203 (2020), https://doi.org/10.1016/j.polymer.2020.122772.
[119] Z. Ciplak, N. Yildiz, A. Calimli, Investigation of graphene/Ag nanocomposites synthesis parameters for two different synthesis methods, Fullerenes, Nanotub. Carbon Nanostruct. 23 (2014) 361–370, https://doi.org/10.1080/1536383X.2014.894025.
[120] H. Kang, Y. Tang, L. Yao, F. Yang, Q. Fang, D. Hui, Fabrication of graphene/natural rubber nanocomposites with high dynamic properties through convenient mechanical mixing, Compos. B Eng. 112 (2017) 1–7, https://doi.org/10.1016/j.compositesb.2016.12.035.
[121] Y. Lin, J. Jin, M. Song, Preparation and characterisation of covalent polymer functionalized graphene oxide, J. Mater. Chem. 21 (2011) 3455–3461, https://doi.org/10.1039/C0JM01859G.
[122] D. Konios, M.M. Stylianakis, E. Stratakis, E. Kymakis, Dispersion behaviour of graphene oxide and reduced graphene oxide, J. Colloid Interface Sci. 430 (2014) 108–112, https://doi.org/10.1016/j.jcis.2014.05.033.
[123] M. Acik, G. Lee, C. Mattevi, A. Pirkle, R.M. Wallace, M. Chhowalla, K. Cho, Y. Chabal, The role of oxygen during thermal reduction of graphene oxide studied by infrared absorption spectroscopy, J. Phys. Chem. C 115 (2011) 19761–19781, https://doi.org/10.1021/jp2052618.
[124] F. Yin, S. Wu, Y. Wang, L. Wu, P. Yuan, X. Wang, Self-assembly of mildly reduced graphene oxide monolayer for enhanced Raman scattering, J. Solid State Chem. 237 (2016) 57–63, https://doi.org/10.1016/j.jssc.2016.01.015.
[125] L.A. Pérez, N. Bajales, G.I. Lacconi, Raman spectroscopy coupled with AFM scan head: a versatile combination for tailoring graphene oxide/reduced graphene oxide hybrid materials, Appl. Surf. Sci. 495 (2019), https://doi.org/10.1016/j.apsusc.2019.143539.
[126] R. Muzyka, S. Drewniak, T. Pustelny, M. Chrubasik, G. Gryglewicz, Characterization of graphite oxide and reduced graphene oxide obtained from different graphite precursors and oxidized by different methods using Raman spectroscopy, Materials 11 (2018) 1050, https://doi.org/10.3390/ma11071050.
[127] D. Li, M.B. Müller, S. Gilje, R.B. Kaner, G.G. Wallace, Processable aqueous dispersions of graphene nanosheets, Nat. Nanotechnol. 3 (2008) 101–105, https://doi.org/10.1038/nnano.2007.451.
[128] V. Loryuenyong, K. Totepvimarn, P. Eimburanapravat, W. Boonchompoo, A. Buasri, Preparation and characterization of reduced graphene oxide sheets via water-based exfoliation and reduction methods, Adv. Mater. Sci. Eng. (2013), 923403, https://doi.org/10.1155/2013/923403 (2013).
[129] X. Qi, T. Zhou, S. Deng, G. Zong, X. Yao, Q. Fu, Size-specified graphene oxide sheets: ultrasonication assisted preparation and characterization, J. Mater. Sci. 49 (2014) 1785–1793, https://doi.org/10.1007/s10853-013-7866-8.
[130] Chaiyakun S. Rattana, N. Witit-anun, N. Nuntawong, P. Chindaudom, S. Oaew, C. Kedkeaw, P. Limsuwan, Preparation and characterization of graphene oxide nanosheets, Proc. Eng. 32 (2012) 759–764, https://doi.org/10.1016/j.proeng.2012.02.009.
[131] J. Wang, G. Fei, Y. Pan, K. Zhang, S. Hao, Z. Zheng, H. Xia, Simultaneous reduction and surface functionalization of graphene oxide by cystamine dihydrochloride for rubber composites, Compos. Appl. Sci. Manuf. 122 (2019) 18–26, https://doi.org/10.1016/j.compositesa.2019.04.018.
[132] Y.C.G. Kwan, G.M. Ng, C.H.A. Huan, Identification of functional groups and determination of carboxyl formation temperature in graphene oxide using the XPS O 1s spectrum, Thin Solid Films 590 (2015) 40–48, https://doi.org/10.1016/j.tsf.2015.07.051.
[133] M. Tian, J. Zhang, L. Zhang, S. Liu, X. Zan, T. Nishi, N. Ning, Graphene encapsulated rubber latex composites with high dielectric constant, low dielectric loss and low percolation threshold, J. Colloid Interface Sci. 430 (2014) 249–256, https://doi.org/10.1016/j.jcis.2014.05.034.
[134] L. Torrisi, L. Silipigni, M. Cutroneo, A. Torrisi, Graphene oxide as a radiation sensitive material for XPS dosimetry, Vacuum 173 (2020), https://doi.org/10.1016/j.vacuum.2020.109175.
[135] R. Lv, Y. Ren, H. Guo, S. Bai, Recent progress on thermal conductivity of graphene filled epoxy composites, Nano Mater. Sci. (2021), https://doi.org/10.1016/j.nanoms.2021.06.001.
[136] M. Kato, S. Guan, X. Zhao, In-situ observation of graphene using an optical microscope, Appl. Surf. Sci. Adv. 6 (2021), https://doi.org/10.1016/j.apsadv.2021.100138.
[137] Z.-S. Wu, W. Ren, L. Gao, B. Liu, C. Jiang, H.-M. Cheng, Synthesis of high-quality graphene with a pre-determined number of layers, Carbon 47 (2009) 493–499, https://doi.org/10.1016/j.carbon.2008.10.031.
[138] B.D. Ossonon, D. Bélanger, Synthesis and characterization of sulfophenyl-functionalized reduced graphene oxide sheets, RSC Adv. 7 (2017) 27224–27234, https://doi.org/10.1039/C6RA28311J.
[139] J. Chen, B. Yao, C. Li, G. Shi, An improved Hummers method for eco-friendly synthesis of graphene oxide, Carbon 64 (2013) 225–229, https://doi.org/10.1016/j.carbon.2013.07.055.
[140] J. Guerrero-Contreras, F. Caballero-Briones, Graphene oxide powders with different oxidation degree, prepared by synthesis variations of the Hummers method, Mater. Chem. Phys. 153 (2015) 209–220, https://doi.org/10.1016/j.matchemphys.2015.01.005.
[141] X. Zhou, J. Zhang, H. Wu, H. Yang, J. Zhang, S. Guo, reducing graphene oxide via hydroxylamine: a simple and efficient route to graphene, J. Phys. Chem. C 115 (2011) 11957–11961, https://doi.org/10.1021/jp202575j.
[142] C. Powell, G.W. Beall, Graphene oxide and graphene from low grade coal: synthesis, characterization and applications, Curr. Opin. Colloid Interface Sci. 20 (2015) 362–366, https://doi.org/10.1016/j.cocis.2015.11.003.
[143] J. Song, X. Wang, C.-T. Chang, Preparation and characterization of graphene oxide, J. Nanomater. 2014 (2014), 276143, https://doi.org/10.1155/2014/276143.
[144] J. Li, X. Zhao, W. Wu, X. Ji, Y. Lu, L. Zhang, Bubble-templated rGO-graphene nanoplatelet foams encapsulated in silicon rubber for electromagnetic interference shielding and high thermal conductivity, Chem. Eng. J. 415 (2021), 129054, https://doi.org/10.1016/j.cej.2021.129054.
[145] A. Das, G.R. Kasaliwal, R. Jurk, R. Boldt, D. Fischer, K.W. Stöckelhuber, G. Heinrich, Rubber composites based on graphene nanoplatelets, expanded graphite, carbon nanotubes and their combination: a comparative study, Compos. Sci. Technol. 72 (2012) 1961–1967, https://doi.org/10.1016/j.compscitech.2012.09.005.
[146] Y. Luo, R. Wang, S. Zhao, Y. Chen, H. Su, L. Zhang, T.W. Chan, S. Wu, Experimental study and molecular dynamics simulation of dynamic properties and interfacial bonding characteristics of graphene/solution-polymerized styrene-butadiene rubber composites, RSC Adv. 6 (2016) 58077–58087, https://doi.org/10.1039/C6RA08417F.
[147] J. Hári, B. Pukánszky, 8 - nanocomposites: preparation, structure, and properties, in: M. Kutz (Ed.), Applied Plastics Engineering Handbook, vols. 109–142, William Andrew Publishing, Oxford, 2011.
[148] J. Wang, K. Zhang, Q. Bu, M. Lavorgna, H. Xia, Graphene-rubber nanocomposites: preparation, structure, and properties, in: S. Kaneko, P. Mele, T. Endo, T. Tsuchiya, K. Tanaka, M. Yoshimura, D. Hui (Eds.), Carbon-related Materials – in Recognition of Nobel Lectures by Prof. Akira Suzuki in ICCE, vol. 1, Springer, New York, 2017, pp. 175–210.
[149] Z. Tang, X. Liu, Y. Hu, X. Zhang, B. Guo, A slurry compounding route to disperse graphene oxide in rubber, Mater. Lett. 191 (2017) 93–96, https://doi.org/10.1016/j.matlet.2017.01.054.
[150] Y. Lin, Y. Chen, Z. Zeng, J. Zhu, Y. Wei, F. Li, L. Liu, Effect of ZnO nanoparticles doped graphene on static and dynamic mechanical properties of natural rubber composites, Compos. Appl. Sci. Manuf. 70 (2015) 35–44, https://doi.org/10.1016/j.compositesa.2014.12.008.
[151] A. Malas, P. Pal, C.K. Das, Effect of expanded graphite and modified graphite flakes on the physical and thermo-mechanical properties of styrene butadiene rubber/polybutadiene rubber (SBR/BR) blends, Mater. Des. 55 (2014) 664–673, https://doi.org/10.1016/j.matdes.2013.10.038.
[152] S. Hao, J. Wang, M. Lavorgna, G. Fei, Z. Wang, H. Xia, Constructing 3D graphene network in rubber nanocomposite via liquid-phase redispersion and self-assembly, ACS Appl. Mater. Interfaces 12 (2020) 9682–9692, https://doi.org/10.1021/acsami.9b22787.
[153] H. Kim, Y. Miura, C.W. Macosko, Graphene/polyurethane nanocomposites for improved gas barrier and electrical conductivity, Chem. Mater. 22 (2010) 3441–3450, https://doi.org/10.1021/cm100477v.
[154] I. Zaman, H.-C. Kuan, Q. Meng, A. Michelmore, N. Kawashima, T. Pitt, L. Zhang, S. Gouda, L. Luong, J. Ma, A facile approach to chemically modified graphene and its polymer nanocomposites, Adv. Funct. Mater. 22 (2012) 2735–2743, https://doi.org/10.1002/adfm.201103041.
[155] J. Wang, B. Liu, Y. Cheng, Z. Ma, Y. Zhan, H. Xia, Constructing a segregated magnetic graphene network in rubber composites for integrating electromagnetic interference shielding stability and multi-sensing performance, Polymers 13 (2021) 3277, https://doi.org/10.3390/polym13193277.
[156] Y. Zhan, S. Hao, Y. Li, C. Santillo, C. Zhang, L. Sorrentino, M. Lavorgna, H. Xia, Z. Chen, High sensitivity of multi-sensing materials based on reduced graphene oxide and natural rubber: the synergy between filler segregation and macro-porous morphology, Compos. Sci. Technol. 205 (2021), 108689, https://doi.org/10.1016/j.compscitech.2021.108689.
[157] C. Heng, T.P. Leng, A.G. Supri, Y.C. Keat, K. Suppiah, Effect of graphene loading on mechanical properties of polyurethane elastomer, Mater. Today Proc. 16 (2019) 1617–1621, https://doi.org/10.1016/j.matpr.2019.06.026.
[158] S. Paszkiewicz, A. Szymczyk, Z. Špitalský, J. Mosnáček, K. Kwiatkowski, Z. Rosłaniec, Structure and properties of nanocomposites based on PTT-block-PTMO copolymer and graphene oxide prepared by in situ polymerization, Eur. Polym. J. 50 (2014) 69–77, https://doi.org/10.1016/j.eurpolymj.2013.10.031.
[159] P. Niu, N. Bao, H. Zhao, S. Yan, B. Liu, Y. Wu, H. Li, Room-temperature self-healing elastomer-graphene composite conducting wires with superior strength for stretchable electronics, Compos. Sci. Technol. 219 (2022), https://doi.org/10.1016/j.compscitech.2022.109261.
[160] X.-J. Shen, S. Yang, J.-X. Shen, J.-L. Ma, Y.-Q. Wu, X.-L. Zeng, S.-Y. Fu, Improved mechanical and antibacterial properties of silver-graphene oxide hybrid/polylactid acid composites by in-situ polymerization, Ind. Crop. Prod. 130 (2019) 571–579, https://doi.org/10.1016/j.indcrop.2019.01.018.
[161] X. Zhao, Y. Li, W. Chen, S. Li, Y. Zhao, S. Du, Improved fracture toughness of epoxy resin reinforced with polyamide 6/graphene oxide nanocomposites

prepared via in situ polymerization, Compos. Sci. Technol. 171 (2019) 180–189, https://doi.org/10.1016/j.compscitech.2018.12.023.
[162] D. Ljubic, M. Srinivasan, R. Szoszkiewicz, I. Javni, Z.S. Petrović, Surface modified graphene/single-phase polyurethane elastomers with improved thermo-mechanical and dielectric properties, Eur. Polym. J. 70 (2015) 55–65, https://doi.org/10.1016/j.eurpolymj.2015.07.008.
[163] X.-B. Fu, X. Tong, J.-C. Yang, G. Zhang, M.-L. Zhang, X.-J. Wang, J. Yang, In situ polymerization preparation and mechanical properties of nanocomposites based on PA10T/10I-block-PEG copolymer and graphene oxide, Nano Mater. Sci. (2021), https://doi.org/10.1016/j.nanoms.2021.09.004.
[164] A. Kiziltas, S. Tamrakar, J. Rizzo, D. Mielewski, Characterization of graphene nanoplatelets reinforced sustainable thermoplastic elastomers, Comp. Part C Open Access 6 (2021), 100172, https://doi.org/10.1016/j.jcomc.2021.100172.
[165] M. Liu, I.A. Kinloch, R.J. Young, D.G. Papageorgiou, Modelling mechanical percolation in graphene-reinforced elastomer nanocomposites, Compos. B Eng. 178 (2019), 107506, https://doi.org/10.1016/j.compositesb.2019.107506.
[166] M. Liu, J.H. Hui, I.A. Kinloch, R.J. Young, D.G. Papageorgiou, Deformation and tearing of graphene-reinforced elastomer nanocomposites, Compos. Commun. 25 (2021), 100764, https://doi.org/10.1016/j.coco.2021.100764.
[167] Y. Su, S. Qiu, J. Wei, X. Zhu, H. Zhao, Q. Xue, Sulfonated polyaniline assisted hierarchical assembly of graphene-LDH nanohybrid for enhanced anticorrosion performance of waterborne epoxy coatings, Chem. Eng. J. 426 (2021), 131269, https://doi.org/10.1016/j.cej.2021.131269.
[168] S. Sahin, A.E. Kavur, S.D. Mustafov, O. Seydibeyoglu, O. Baser, Y. Isler, C. Guzelis, Spatiotemporal chaotification of delta robot mixer for homogeneous graphene nanocomposite dispersing, Robot. Autonom. Syst. 134 (2020), 103633, https://doi.org/10.1016/j.robot.2020.103633.
[169] H. Kasım, A.N. Aldeen, A. Onat, İ. Saraç, B. Engin, M. Yazıcı, Investigation of the crack propagation in the graphene/synthetic rubber nanocomposite materials with DIC technique, Period. Polytech. Chem. Eng. 66 (2022) 192–204, https://doi.org/10.3311/PPch.19079.
[170] A. Mohamed, T. Ardyani, S. Abu Bakar, M. Sagisaka, Y. Umetsu, J.J. Hamon, B.A. Rahim, S.R. Esa, H.P.S. Abdul Khalil, M.H. Mamat, S. King, J. Eastoe, Rational design of aromatic surfactants for graphene/natural rubber latex nanocomposites with enhanced electrical conductivity, J. Colloid Interface Sci. 516 (2018) 34–47, https://doi.org/10.1016/j.jcis.2018.01.041.
[171] W. Xing, H. Li, G. Huang, L.-H. Cai, J. Wu, Graphene oxide induced cross-linking and reinforcement of elastomers, Compos. Sci. Technol. 144 (2017) 223–229, https://doi.org/10.1016/j.compscitech.2017.03.006.
[172] F. Asai, T. Seki, Y. Takeoka, Functional polymethacrylate composite elastomer filled with multilayer graphene and silica particles, Carbon Trends 4 (2021), 100064, https://doi.org/10.1016/j.cartre.2021.100064.